

Slow Spreading Ridges of the Indian Ocean: An Overview of Marine Geophysical Investigations

K. A. Kamesh Raju*, Abhay V. Mudholkar, Kiranmai Samudrala

CSIR-National Institute of Oceanography, Dona Paula, Goa – 403004, India

*Corresponding author: kamesh@nio.org

ABSTRACT

Sparse and non-availability of high resolution geophysical data hindered the delineation of accurate morphology, structural configuration, tectonism and spreading history of Carlsberg Ridge (CR) and Central Indian Ridges (CIR) in the Indian Ocean between Owen fracture zone at about 10°N, and the Rodriguez Triple Junction at ~25°S. Analysis of available multibeam bathymetry, magnetic, gravity, seabed sampling on the ridge crest, and selected water column data suggest that even with similar slow spreading history the segmentation significantly differ over the CR and CIR ridge systems. Topography, magnetic and gravity signatures indicate non-transform discontinuity over CR and suggest that it has relatively slower spreading history than CIR. Magmatic and less magmatic events characterize CR and CIR respectively and well defined oceanic core complex (OCC) are confined only to segments of the CIR. The mantle Bouguer anomaly signatures over the ridges suggest crustal accretion and pattern of localized magnetic anomalies indicate zones of high magnetization coinciding with the axial volcanic ridges. Geophysical investigations / thermal plumes in the water column, have brought out two new hydrothermal vents over CR and one vent indication over the CIR. The analysis of the tectonic and magmatic character of the CR and CIR based on the available high resolution data suggests that both these slow spreading ridge sections have the potential to host high temperature active hydrothermal vents and need to be investigated by AUV and ROV experiments to identify the causative mechanism of these vents and their association with unique seafloor and sub-seafloor deep-sea ecosystems. These ridges hold great promise of mineral resources.

INTRODUCTION

Mid-oceanic ridges are the sites of abundant volcanic activity and generation of new oceanic crust. The ridge system exerts major influence on the evolution of the solid earth mainly in terms of manifestation of sea floor relief controlling plate motions, modulating crustal weak zones, chemically/thermally altering the entire oceanic lithosphere, producing mineralized zones in the crust and supporting unique forms of life. (Stein and Stein, 1994; Fisher, 2003) The interplay of tectonic and magmatic processes greatly controls the emplacement and evolution of the seafloor. Transform faults, ridge-transform intersection highs (Wilson, 1965; Turcotte, 1974; Sandwell, 1986), detachment faults and oceanic core complex (OCC) formation (Tucholke et al. 1998, 2008; Escartin et al. 2008) are some of the important features that modulate and shape the ridges and the nature of the young oceanic crust. The manifestation of the oceanic crustal evolution can be seen as segmentation (Macdonald et al., 1988; Macdonald et al., 1991), along axis crustal thickness variations (Lin et al., 1990; Lin and Morgan, 1992; Tolstoy et al., 1993), and emplacement of OCCs. The study of mid-ocean ridges provides us an opportunity to understand the processes of oceanic crust generation and deep-sea mineral formation. Detailed investigation of few ridge segments out of the ~60,000 km long mid-ocean-ridge system has provided

new insights that did not agree with our simple conceptual models, there by stressing the importance of detailed study of the ridge system.

Technological advances in deep-submergence instrumentation, autonomous underwater vehicles (AUVs), remotely operated vehicles (ROVs) and manned submersibles like Alvin, MIR, Nautile etc., greatly helped our ability to examine the ridge crest region in detail and lead to new discoveries of vent fields and seafloor and sub-seafloor ecosystems. The exploration of mid-ocean ridges is an extremely challenging and rewarding field of multidisciplinary science that provides opportunities to study both basic and applied aspects associated with oceanic crustal generation processes, and deep sea ecosystems. Exploration remains necessary to know the diversity and variability in terms of time and space in the complex process of crustal generation and associated phenomenon. A review (Hannington et al., 2011) of the status of exploration provides new insights about the frequency of occurrence of active hydrothermal vent systems (Figure 1).

The mid-ocean ridges in the Indian Ocean comprise of Carlsberg ridge (CR), Central Indian Ridge (CIR), South West Indian Ridge (SWIR), and South East Indian Ridge (SEIR) systems. The CIR, SWIR and SEIR meet at the Rodriguez Triple Junction (RTJ) forming an inverted Y shaped ridge system (Figure 2).

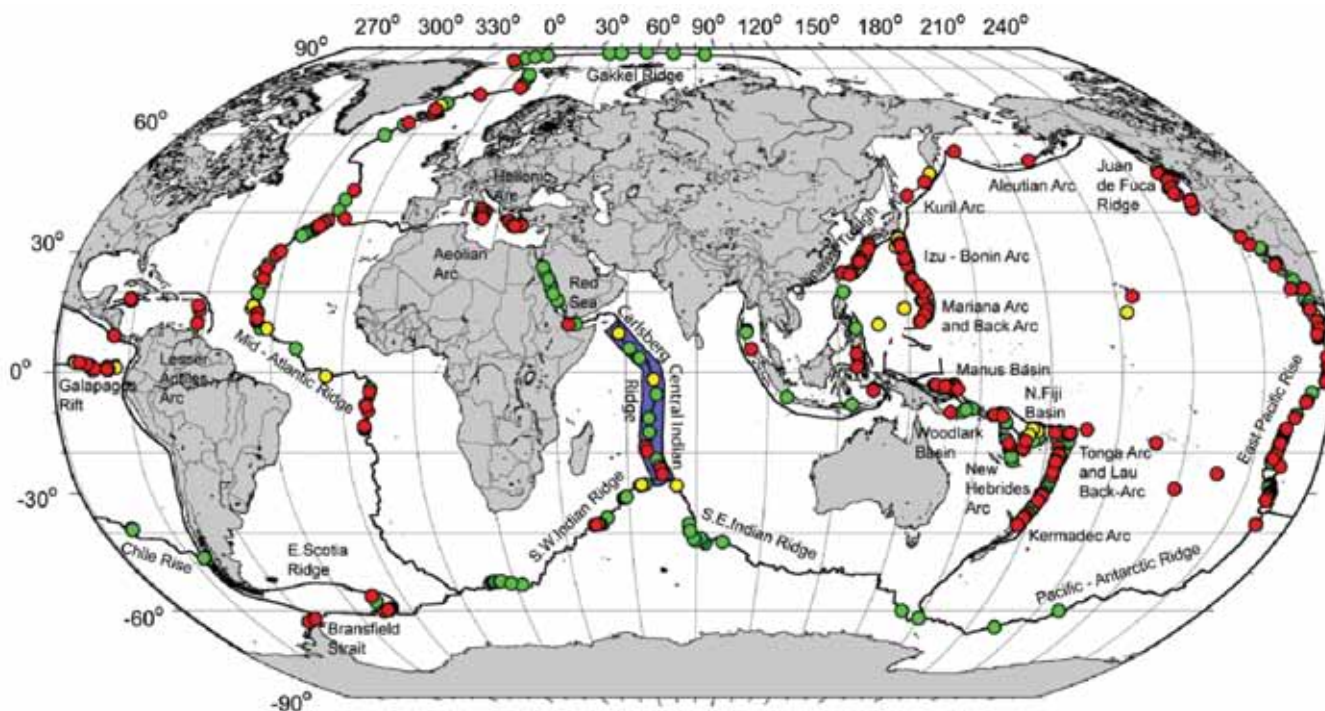


Figure 1. Global distribution of active, inferred active (unconfirmed) and inactive submarine hydrothermal vent fields. The red color symbols denote the active vent fields, green color symbols represents the active unconfirmed fields and the yellow represents inactive vent fields (after Beaulieu, 2010). The purple shaded region covering Carlsberg and Central Indian Ridges is the study area.

The Indian ridge program initiated in 2002 by the CSIR-National Institute of Oceanography focused on the CR and CIR sections of the mid-ocean ridge system in the Indian Ocean. These studies have provided insights into the tectonic and magmatic processes along these slow spreading ridges (Mudholkar et al., 2002; Kamesh Raju et al., 2008; Kamesh Raju et al., 2012) and provided evidence for two vent locations over the Carlsberg Ridge in the northern Indian Ocean (Ray et al., 2012), and a new plume location over the Central Indian Ridge segment, around 10°48'S. In this brief overview we focus on the geophysical signatures of the Carlsberg and Central Indian Ridge sections, north of Rodriguez triple junction, and deliberate upon the processes of ridge segmentation and evolution.

MORPHOLOGY, GEOLOGY AND GEOPHYSICAL SIGNATURES OF MID OCEAN RIDGE SYSTEMS

The distinct topographic fabric of the ridge and its segmentation largely represent the temporal and spatial interplay of two primary processes, viz., i) magmatic process that provides the melt to form new oceanic crust, and ii) tectonic process during which deformation, faulting and dismemberment of the crust takes place. It is, therefore, important to identify the contribution of these processes

to understand the finer scale evolution of the ridge system. High-resolution mapping efforts over the mid-ocean ridges world-over revealed the existence of new families of ridge axis discontinuities based on high resolution topographic fabric of the ridge crest region. These studies have shown that the ridge axis discontinuities primarily divide the ridge into smaller segments with varied topographic expressions as a consequence of variations in the crustal accretion (Macdonald and Fox, 1990; Shaw, 1992; Sinton and Detrick, 1992).

Extensive investigations carried out over East Pacific Rise (EPR) and over the segments of MAR have provided insights into the segmentation pattern and accretionary processes of the fast and slow spreading ridge systems (Macdonald et al., 1991; Scheirer and Macdonald, 1993; Sempere et al., 1990, 1993; Smith and Cann, 1993; Gente et al., 1995; Goslin et al., 1999). Recent investigations over the very-slow South West Indian Ridge (German et al., 1998; Sauter et al., 2001; Dick et al., 2003) and the ultra-slow Arctic Ridges (Cochran et al., 2003; Michael et al., 2003) have enhanced our understanding of the architecture and accretionary processes of the very-slow and ultra-slow spreading mid-ocean ridges.

The discovery of first hydrothermal vent in 1977 (Corliss et al., 1979) and subsequent discovery of many active vent sites along the fast, intermediate, slow, very-slow

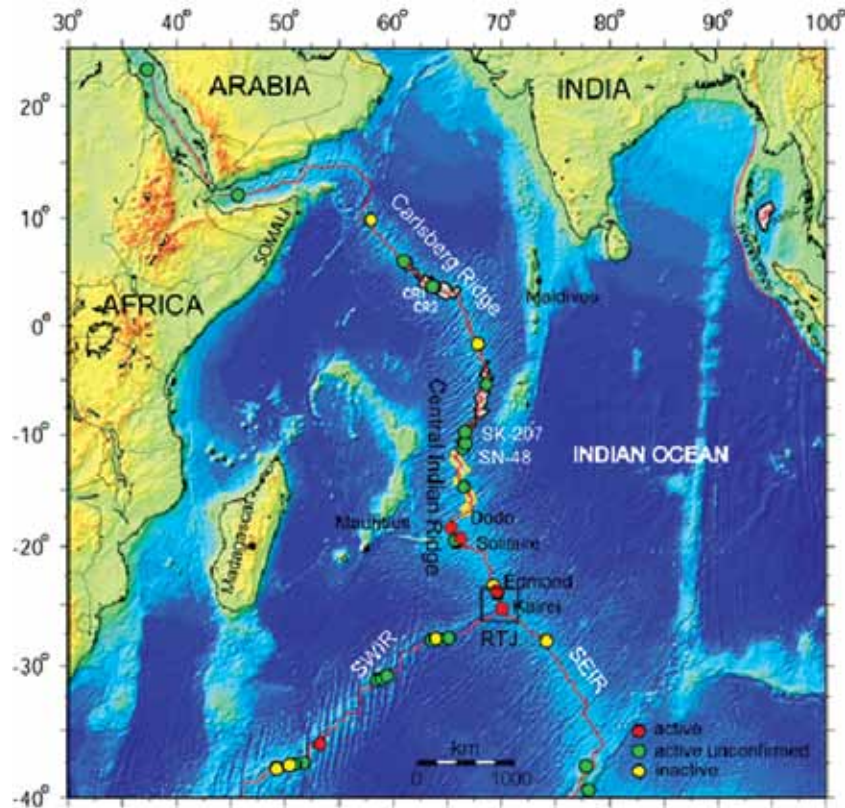


Figure 2. Indian Ocean Ridge systems with seafloor topography (Smith and Sandwell, 1997) along with confirmed (red), inferred (unconfirmed) active (green) and inactive (yellow) vent fields in the Indian Ocean. Shaded box with black outline denotes the study areas covered by CSIR-NIO. Shaded box with white outline denotes the area covered by Son et al. (2014), the black box encompassing RTJ represents the area of detailed investigations (Honsho et al., 1996; Sauter et al., 1996; Mendel et al., 2000; Hashimoto et al., 2001; Van Dover et al., 2001; Tamaki et al., 2010).

and ultra-slow spreading centers all over the global ridge systems and plate boundaries (Beaulieu, 2010; Beaulieu et al., 2013) demonstrate the widespread prevalence of these features over mid-ocean ridges with varied spreading rates (Figure 1). The recent discovery of the deepest vent field in Cayman Trough (German et al., 2010) has added to the global repository of the known active vent fields. The mid-ocean ridges have also become important targets for the massive sulphide deposits associated with the hydrothermal vents. The recent interest in the exploration of ridges has been driven by the expectations of mineral resources that are associated with the massive sulphide deposits at the hydrothermal vent sites.

The Ridge-Transform Intersections (RTIs) are important structural features along the mid-ocean ridge crest region; these are more prominent over slow spreading ridges. Some of these RTI highs are classified as oceanic core complexes (OCCs) when they are associated with detachment faults. The absence of transform faults over a long section of the CR is conspicuous. Consequently only two RTIs have been documented between the 62°E to 66°E. In contrast, seven prominent RTIs have been identified on the CIR (Kamesh Raju et al., 2012).

GEOLOGICAL SETTING - INDIAN OCEAN RIDGE SYSTEMS

Nearly 4000 km long section of the mid-ocean ridge system in the Indian Ocean, comprising of CR and CIR sections between Owen fracture zone at about 10°N, and the Rodriguez Triple Junction at ~25°S, remained poorly explored with high resolution geophysical tools. However, a limited region near the Rodriguez triple junction encompassing the CIR segment has been well explored leading to the discovery of four active vents (Honsho et al., 1996; Sauter et al., 1996; Mendel et al., 2000; Hashimoto et al., 2001; Van Dover et al., 2001; Tamaki et al., 2010). The meager occurrence of active vent fields in the Indian Ocean ridges (Figure 2) highlight the paucity of known active fields or confirmed plumes over the CR and CIR segments. These limited findings have adversely impacted many aspects of hydrothermal research, especially the biogeography of deep-sea vent fauna. The paucity of available samples from the Indian Ocean is a major hindrance in assessing the role of the Indian Ocean ridges as migration corridors of hydrothermal vent fauna between the Pacific and Atlantic vent fields.

Carlsberg Ridge

The Carlsberg Ridge (CR) in the northwest Indian Ocean defines the plate boundary between the Indian and Somalian plates (McKenzie and Sclater, 1971; Royer et al., 1989). The Carlsberg Ridge initiates at the Owen fracture zone near 10°N and extends to the Central Indian Ridge near the equator (Figure 2). The CR is a typical slow spreading ridge with an average spreading rate of 22 to 32 mm/yr, a V-shaped rift valley, and a wide valley floor. Magmatic and sparsely magmatic segments, non-transform discontinuities (NTDs) and a few well-defined transform faults (TFs) characterize the CR (Kamesh Raju et al., 2008).

Central Indian Ridge

The Central Indian Ridge (CIR) extending from equator to the Indian Ocean triple junction at 25°S is a slow spreading mid-ocean ridge (Figure 2). Basin scale regional marine geophysical investigations focused on tectonic evolution of the Indian Ocean (Vine and Matthews, 1963; McKenzie and Sclater, 1971; Schlich, 1982), and the plate reconstruction models (Royer et al. 1989; DeMets et al. 1994), have provided broad scale geometry of this ridge. The spreading rates range from 26 to 40 mm/yr (Kamesh Raju et al., 2012, Son et al., 2014); well defined core complex structures have been documented over this ridge.

DATA TYPES AND METHODS

The marine geophysical data acquired during the investigations of the CR and CIR segments consist of magnetics, gravity, multibeam swath bathymetry, deep-tow and seafloor photography. The seabed sampling data consisted of dredge, spade core, gravity core, and TV-grab samples. The water column data has been obtained by CTD. MAPRs (Miniature Autonomous Plume Recorders) that record temperature, turbidity and Oxidation Reduction Potential (ORP) parameters have been employed during the exploration. AUV and submersible dives have been conducted over the segments of the CIR.

MB-System (Caress and Chayes, 1995) was used to process the multibeam bathymetry data collected by CSIR-NIO. The total magnetic field data compiled from CSIR-NIO data base were reduced by subtracting the IGRF filed model (IAGA, 2000). Satellite derived topography (Smith and Sandwell, 1997) and gravity (Sandwell and Smith, 1997) have been used to visualize the configuration of the mid-ocean ridge system. GMT (Wessel and Smith, 1991) software was used for plotting and presentation of the data. Seafloor spreading magnetic model studies have been carried out to identify the magnetic anomalies and to assign

the spreading rates. Synthetic anomaly profile is generated using the time scale of Cande and Kent (1995) by assuming 500 m thick blocks with 0.01 A/m magnetization.

MORPHOTECTONICS

The ridge systems in the north Indian Ocean are least explored with respect to surveys with modern mapping tools. First results of detailed segment scale investigations carried out over parts of the CIR using modern tools such as Gloria sidescan and multibeam bathymetry were provided by Parson et al., (1993), Briais (1995) and Kamesh Raju et al. (1997). The magnetic and bathymetric investigation results of Drolia et al. (2000) have provided tectonic implications of the ridge segmentation over a part of the CIR. Insights into the influence of diffuse plate deformation zone on the seafloor fabric and its implications were discussed (Drolia and DeMets, 2005) based on multibeam bathymetry and magnetic data.

Ridge Segmentation

a. Carlsberg Ridge

The segmentation pattern of the Carlsberg Ridge between 62°20'E and 66°20'E (Figure 3) has been investigated using swath bathymetry and magnetic data (Kamesh Raju et al., 2008). Swath bathymetry revealed high resolution topography of the ridge. The CR, characterized by rugged topography, steep valley walls and wide rift valley floor, and a propagating ridge segment representing the traits of a slow spreading ridge. A mantle Bouguer anomaly low of ~50 mGal (Kamesh Raju et al., 1998) indicates focused mantle upwelling and thick crust underneath this propagating ridge section. There is only one first order discontinuity caused by a well-defined transform fault and fracture zone along a long section of the CR between 57°E and 65°E (Figure 3). The ridge in general is oriented in a NW-SE direction; the gradual bend in the ridge axis is accommodated by non-transform discontinuities and along-axis bathymetric deeps (Figure 3). Based on characters related to topography, the off-axis trace of the discontinuities, and the presence or absence of ridge-parallel topographic fabric, the ridge has been divided into four segments, referred as segments I to IV (Kamesh Raju et al., 2008). There are significant variations in the width of the valley floor along the ridge axis. Segment II (63°10' to 63°18'E) is the most distinctive segment. It has the widest (maximum width ~25 km) and the deepest (maximum depth ~4700 m) axial valley floor, and is characterized by blocky topographic fabric and off-axis highs (Figure 3). It has been well documented that slow-spreading ridges are characterized by shallow segment centers and deeper segment ends (Kuo and Forsyth, 1988; Lin et al., 1990; Shaw, 1992).

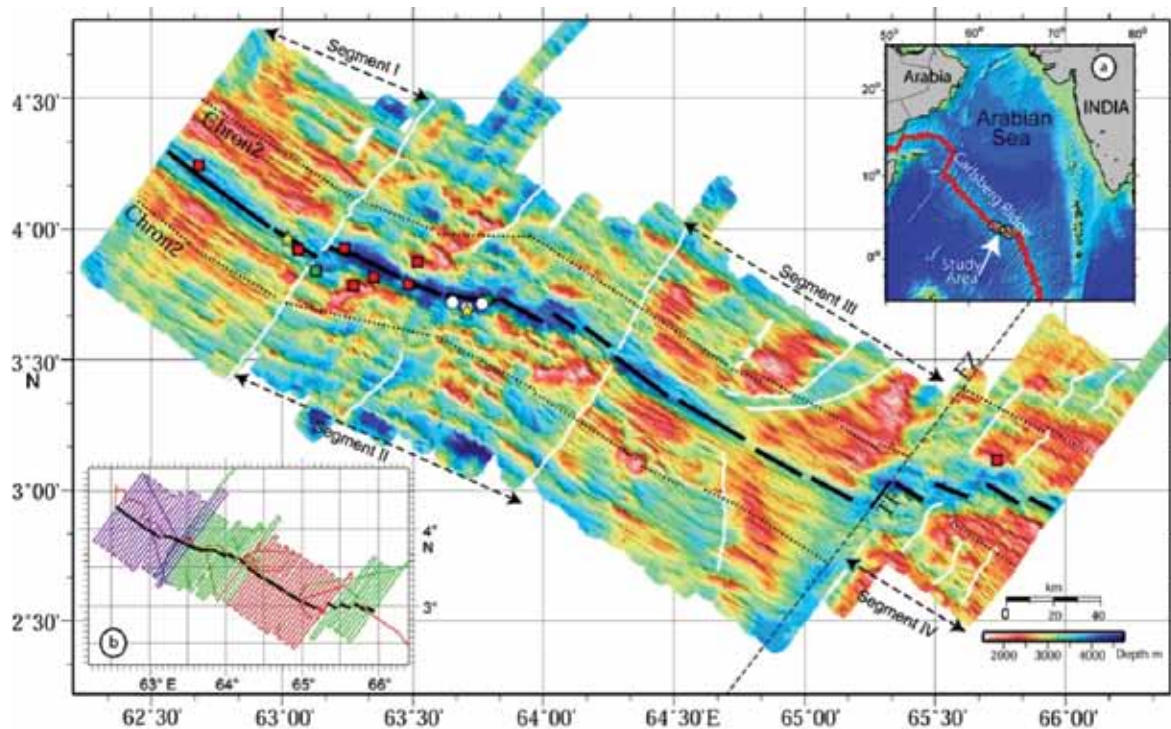


Figure 3. Swath bathymetry map of a section of the Carlsberg Ridge along with sample locations and ridge segments (after Kamesh Raju et al., 2008). Red squares indicate basalts, green color indicate ultramafics, Star symbol denotes the TV-grab sample location. Recently discovered inferred active vent fields are indicated by white filled circles. a. Index map showing the Carlsberg ridge in the Arabian Sea b. ship tracks.

b. Central Indian Ridge

The 750 km long section of the CIR between 3°S to 11°S is characterized by rugged topography, steep valley walls, and well defined rift valley floor, all characteristics of slow spreading ridges. The spreading rates are slightly higher than the slow spreading Carlsberg Ridge (Kamesh Raju et al., 2008) and the ridge is characterized by well defined spreading segments bounded by transform faults. The identified ridge segments are named from I to P and the corresponding fracture zones are labeled with a pre-fix “FZ-” Ridge segments separated by non-transform discontinuities are labeled with numbered alphabet (e.g. K1, K2, and M1, M2) (Figure 4).

The along axis valley floor depth varied from 2743 m to 4638 m with the average depth of the rift valley floor at 3500 m. The segment L has the shallowest rift valley at 2743 m and is conspicuous in its character compared to other segments, the rift valley almost disappears at the center of this segment (Figure 4). Excluding the segment L, the shallowest axial depth of each segment is in the range of 3500 - 4000 m. Full spreading rate of 38 mm/yr was observed over the segment L. Of the identified 12 segments majority of the segments have faster spreading rates over the north-eastern flank. There appears to be no apparent correlation between axial valley depth and the spreading

rates (Kamesh Raju et al., 2012). The deepest portion of the transform valley reached a depth of 6300 m at the Vema transform. Recent systematic surveys between 8°S to 17°S over the CIR identified seven segments with 35-40 mm/yr spreading rate (Son et al., 2014). These studies have reported hydrothermal plume signatures from all the seven segments.

Magmatic and sparsely magmatic ridge segments

The studies of ridge crest morphology over the slow spreading ridges have shown that there is discernable relationship between the rift valley morphology and the crustal accretion and extension processes. Based on extensive study of the ridge crest topography it was suggested that the rift valley morphologies are a consequence of competing magmatic and tectonic (less magmatic extension) processes and are related to magma supply (Perfit and Chadwick, 1998). Segments with narrow and shallow V-shaped rift valley are interpreted to be magmatic, this interpretation is supported by the presence of near circular mantle Bouguer anomaly lows observed over these ridge segments indicating focused mantle upwelling resulting in thicker crust (Kuo and Forsyth, 1988; Lin et al., 1990; Tolstoy et al., 1993; Fujimoto et al., 1996; Maia and Gente, 1998). The ridge segments with deeper and wider U-shaped valley

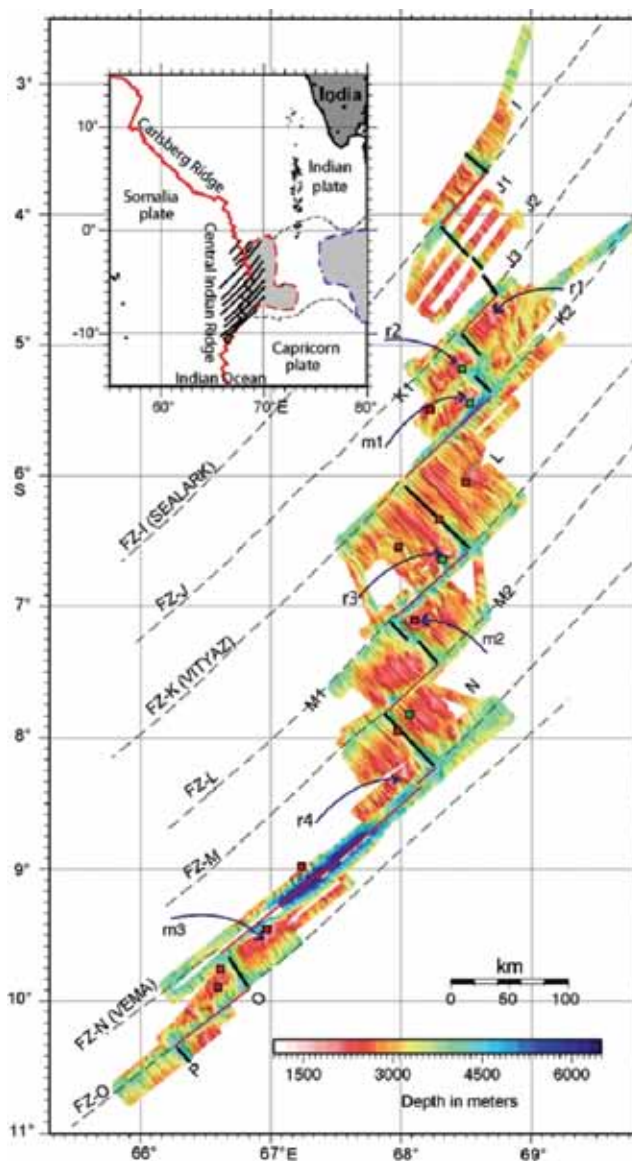


Figure 4. Swath bathymetry map of a section of the Central Indian Ridge (CIR). Square symbols denote the dredge sampling locations, red indicates fresh basalts and green indicates recovery of mantle derived rocks. m1, m2 and m3 indicate the identified megamullion features. r1, r2, r3, r4 indicate ridge-transform intersection highs. FZ-I to FZ-O represent the Fracture zones. Inset shows the Indian Ocean Ridge system along with the broad deformation zone (DeMets et al., 1994), the shaded regions with red and blue outlines within the deformation zone represent the divergent and convergent domains (Royer and Gordon, 1997) respectively (after Kamesh Raju et al., 2012).

configuration with rough topographic fabric are considered to be sparsely magmatic with dominant tectonic extension. Based on these criteria, the ridge segments of the Carlsberg and Central Indian Ridges are classified as magmatic and less magmatic segments.

Magmatic and less-magmatic segments of the Carlsberg Ridge

Segments I and III (Figure 3) are considered as magmatic sections of the ridge based on the along axis and off-axis

topographic character. Prominent axial volcanic ridges (AVRs) ranging in length of 16 to 23 km are documented in this segment. The AVRs are the principal sites of lava extrusion (Macdonald and Luyendyk, 1977). Prominent AVRs were identified in wide-ranging morphologies and structures over the northern MAR segments (Sempere et al., 1990; Kong et al., 1988; Smith and Cann, 1993). It is observed that these AVRs get fused to the valley walls during the course of evolution of the spreading segment. The rift valley floor along the CR widens at the NTD (03°52'N; 63°10'E) and peridotites along with gabbros

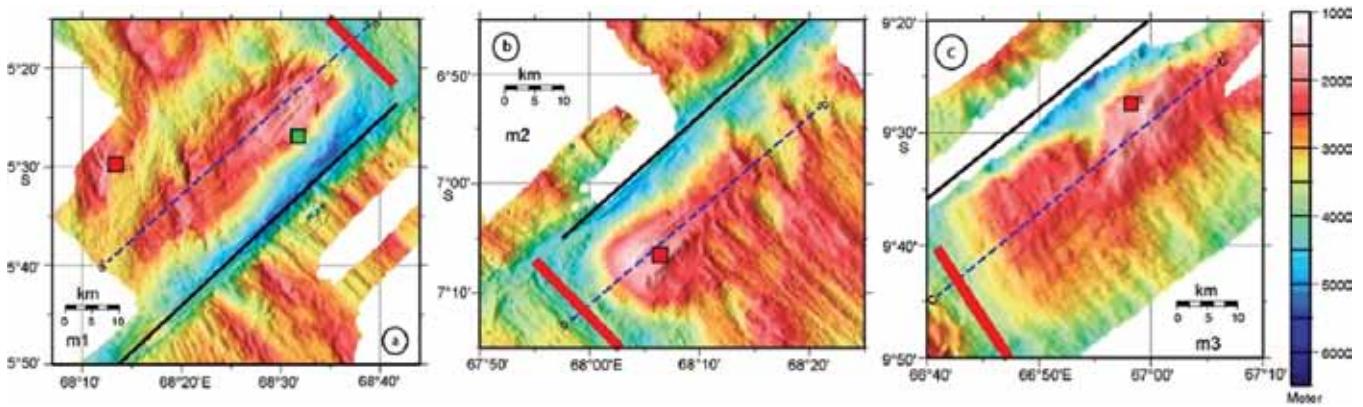


Figure 5. Megamullion structures identified at the inside corners of the Central Indian Ridge segments. a-c represent the detailed multibeam bathymetry of the identified megamullion structures m1, m2 and m3. Ridge axis and transform faults are indicated by thick red and black lines respectively. Seabed sample locations are indicated by square symbols (modified after Kamesh Raju et al., 2012).

were recovered from the base of the valley wall in this region (Figure 3) suggesting a thinner crust exposing the mantle rocks.

Segment III is characterized by a linear section of the ridge with a relatively shallow rift valley. Smooth and elevated topography is observed on the flanks of these segments (Figure 3) suggesting magmatic phase of accretion. Based on morphology, mantle Bouguer anomalies and seismic signatures, the shallower mid sections of the ridge segments are considered as regions of enhanced mantle upwelling (Purdy and Detrick, 1986; Kuo and Forsyth, 1988; Sempere et al., 1990; Lin et al., 1990; Kamesh Raju et al., 1997). The ridge segment is shallowest in the middle at about $3^{\circ}10'N$ latitude and $64^{\circ}48'E$ longitude (Figure 3) reaching to 2900 m, whereas at the ends of the segment, depths reach 4000 m. The rift valley is relatively narrow, having a minimum width of 5 km at the shallowest part.

Segments II and IV (Figure 3) represent sparsely magmatic sections of the ridge. Segment II constitutes a broad deformed zone defining a bend in the ridge axis. The chaotic, blocky topographic fabric with less symmetry with respect to the ridge axis characterizes this segment. The deformation of the seafloor can be seen off axis. The rift valley is about 25 km wide around $3^{\circ}45'N$ latitude and $63^{\circ}45'E$ longitudes. Mantle derived serpentinites were recovered near this region (Figure 3). The thin-crust domains were found to have rugged topography (Cannat et al., 1995). Recovery of mantle derived ultramafics at $15^{\circ}N$ region of MAR was attributed to low magma supply (Cannat et al., 1997). Segment IV consists of an en-echelon pattern of short ridges east of the transform fault at $65^{\circ}18'E$ (Figure 3). Prominent AVR rise to about 800 m from the inner valley floor on either side of the spreading axis.

Magmatic and less-magmatic segments of the Central Indian Ridge

The multibeam bathymetry data over the recently surveyed section of the CIR has shown wide variation over the along axis and across axis morphotectonic character within and between the ridge segments. These variations are similar to the northern and southern MAR and the Carlsberg Ridge segments (Karson et al., 1987; Grindlay et al., 1992; Fox et al., 1991; Sempere et al., 1993; Kamesh Raju et al., 2008).

There are two sections that encompass non-transform discontinuities bounding the segments K1, K2 and M1, M2 (Figure 4). These sections appear to be less magmatic with rugged flank topography, deep and wide rift valley floor. Oblique abyssal hill fabric is noticed at $5^{\circ}S$ on the NE flank of the segment K1 (Figure 4).

Segments L and N display characteristics of magmatic sections. The segment L has the shallowest valley floor reaching to 2743 m in the middle of the segment, suggesting thicker crust due to local upwelling of magma. The Segment N displays well defined ridge parallel topographic fabric. A relative mantle Bouguer anomaly (MBA) low observed in the middle of this segment N was suggested to be the consequence of crustal accretion due to magmatic activity (Kamesh Raju et al., 1997).

The overall segment lengths varied from 18 to 75 km, the shortest is segment O and the longest being the segment L with shallow rift valley floor. Segments L and N have narrow and shallow rift valleys and have lengths of 75 km and 60 km respectively. The segments L and N can be suggested to be undergoing magmatic phase of accretion based on similarities in the topographic fabric, rift valley morphology, and the presence of mantle Bouguer anomalies. The segments I, J, K, M, and O characterized by well defined wide rift valleys with deep valley floor that

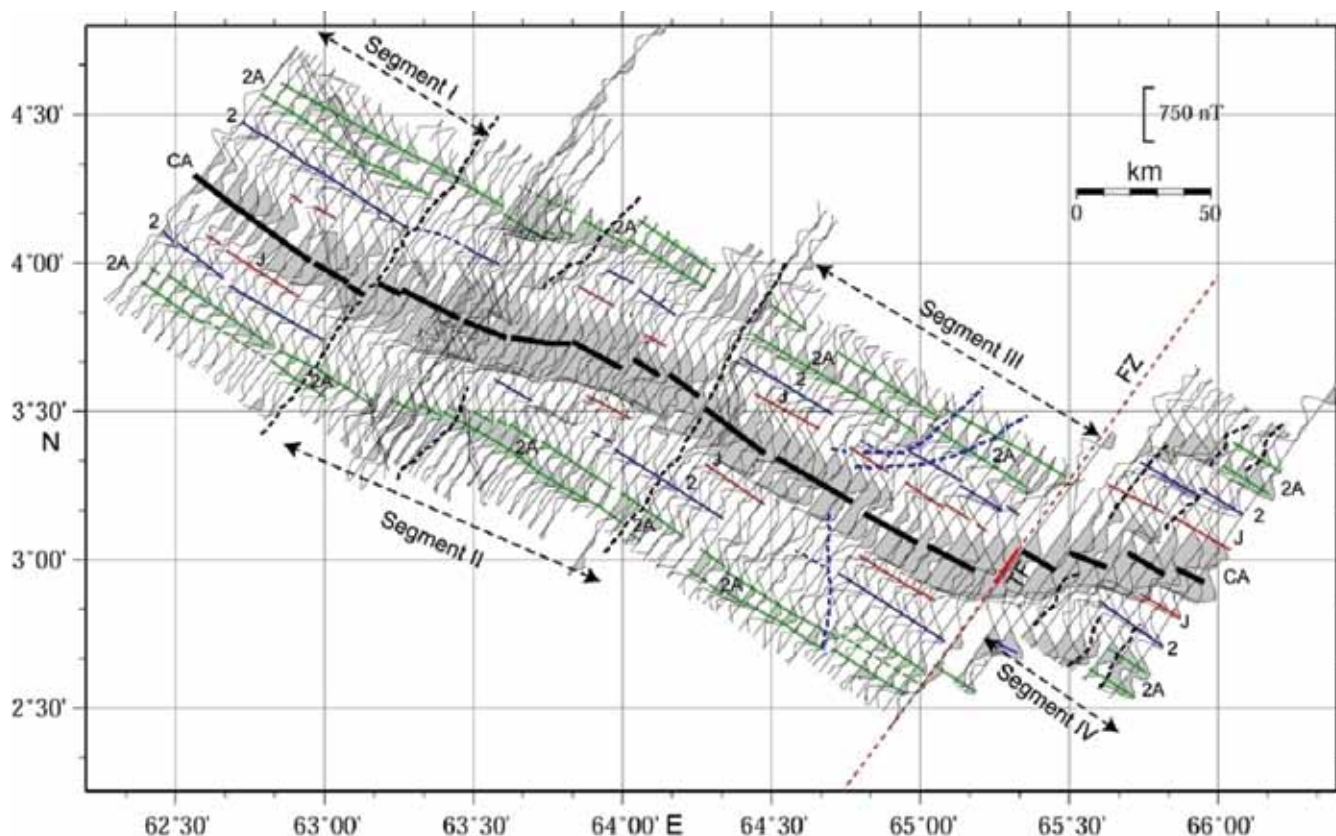


Figure 6. Magnetic anomalies over a section of the Carlsberg Ridge. Segments and the ridge axis delineated based on topography are shown. Thin lines with numbers at the end denote the identified magnetic anomalies. CA represents central anomaly. Dashed lines represent the segment boundaries and the pseudofaults identified based on swath bathymetry.

varied between 3500 to 4500 m appear to be experiencing less magmatic or sparsely magmatic phase of accretion.

RTI and Megamullion features of the Central Indian Ridge

Even though seven prominent RTI highs at the inside corners of the segments are seen on the swath bathymetry (Figure 4), only three of these features are recognized as OCCs based on the diagnostic geomorphological characteristics defined by Tucholke et al. (1998). These OCCs, also called as megamullion structures are suggested to have formed due to the exhumation of mantle rocks through detachment faults. The identified megamullions are named as m1 to m3 (Figure 4). These are located near to the transforms that are bounded by sparsely magmatic ridge segments. The prominent dome shaped structures varied in length 35 to 39 km and exist along the flow-lines parallel to the transform zone. Corrugations that align perpendicular to the ridge are prominent on m1 and m2 (Figures 5a and 5b), these are less prominent on m3 (Figure 5c). The m1 megamullion structure, also known as Kurchatov seamount in some hydrographic maps, was

first identified as a megamullion structure by Drolia and DeMets (2005) and is known as Vityaz megamullion. Fresh basalts and serpentinized peridotites were recovered from dredge hauls over this megamullion structure.

GEOPHYSICAL SIGNATURES

Magnetic anomalies and magnetization

a. Carlsberg Ridge

Along-track plot of the magnetic anomalies (Figure 6) depict well-defined central anomaly that displays variations along the axis and identifiable magnetic lineations on either side of the ridge axis. Seafloor spreading magnetic model studies have been carried out to identify the magnetic anomalies and to assign the spreading rates. Synthetic anomalies are generated with variable spreading rates, using the time scale of Cande and Kent (1995), and assuming 500 m thick blocks with 0.01 A/m magnetization. The model studies (Kamesh Raju et al., 2008) indicate variable and asymmetric spreading rates ranging from 22 mm/yr to 32 mm/yr.

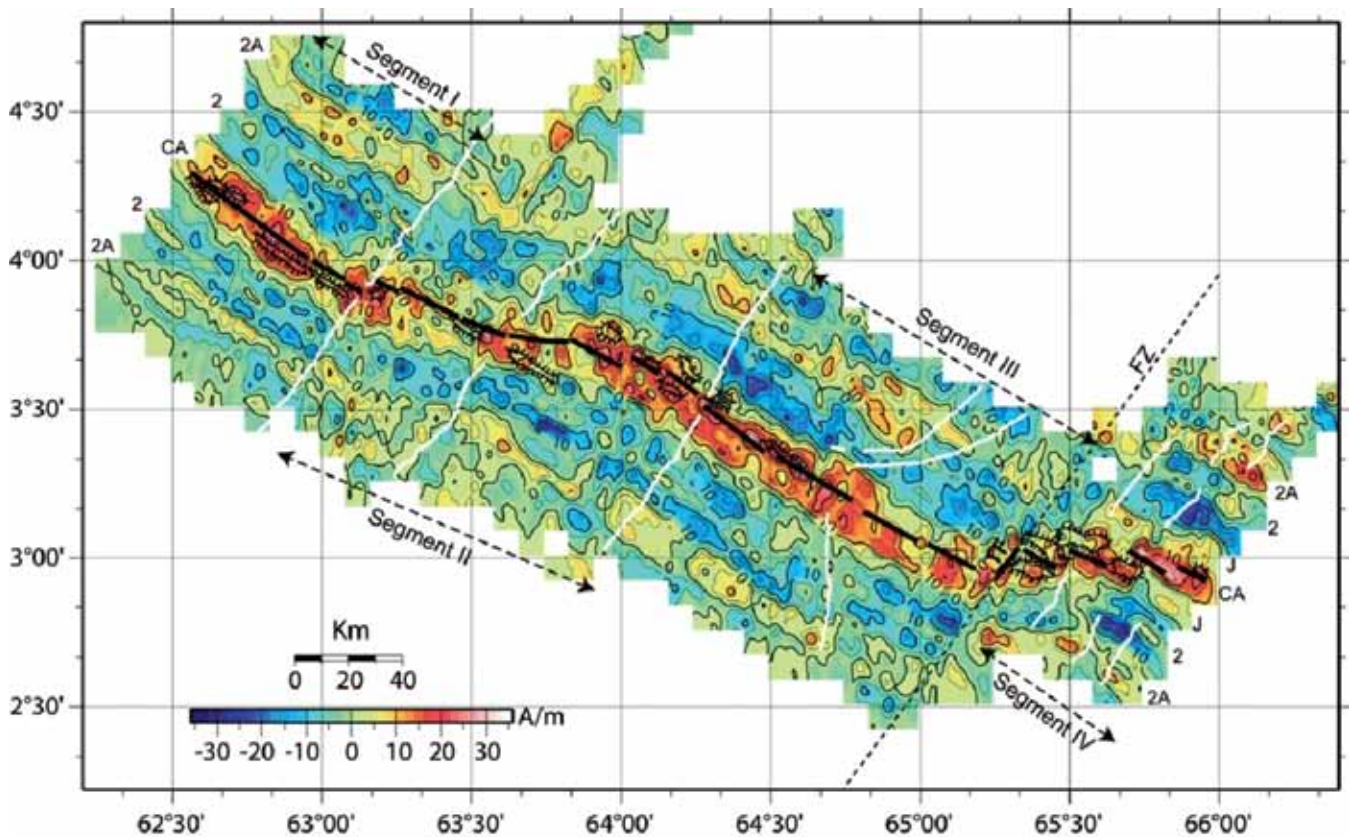


Figure 7. Magnetic inversion solution map of a part of the Carlsberg Ridge computed by using the close grid total magnetic intensity and multibeam bathymetry data.

Over the segment I, the linear trend of anomalies can be correlated with the ridge-parallel topographic fabric. The width of the central anomaly varies between 20-30 km and the amplitude from 150-330 nT. High amplitude and high wave-length anomalies are observed near NTD. Serpentinites and peridotites were recovered in a dredge sample from the rift valley wall at the NTD. The average half spreading rate in this segment is 12 mm/yr to the southwestern flank, and 15 mm/yr to the northeastern flank (Kamesh Raju et al., 2008). The bend in the ridge axis in Segment II is reflected in the magnetic signature. The central anomaly is generally wide in this segment, ranging from 29 to 36 km (Figure 6), with amplitudes ranging from 180 to 400 nT. The magnetic lineations of J and 2 are not continuous while anomaly 2A is well documented and can be correlated. The off-axis topographic fabric does not show ridge parallel fabric and appears to be disturbed until anomaly 2A. The ridge-parallel fabric can be seen beyond anomaly 2A. The seafloor spreading magnetic model studies carried out over the profiles suggest asymmetric spreading with higher spreading rates over the NE flank for the segments I, II and III. The spreading rate is higher over the SW flank for the Segment IV east of the

transform fault.

In Segment III, offsets of the order of 4 km are documented in the magnetic lineations (Figure 6), which correspond to the oblique trending topographic fabric (Figure 3) observed here. The topographic fabric and the magnetic signatures suggest ridge propagation (Hey et al., 1980). The magnetic lineations show offsets corresponding to the bathymetric lineations; these offsets are better developed on the north-eastern ridge flank among the anomalies 2 and 2A with an offset distance of about 4 km (Figure 6). On the south western flank, a noticeable offset is observed only across the magnetic lineation 2A, the magnetic lineation representing anomaly 2 terminates corresponding to the flank topographic high. Magnetic lineations show prominent offsets across the transform fault and the fracture zone. High intensity magnetic anomalies are noticed over the AVRs identified from swath bathymetry. Spreading rates determined from seafloor-spreading model studies over Segment III indicate average half spreading rates varying from 11 mm/yr to 15.5 mm/yr (Kamesh Raju et al., 2008).

Segment IV is characterized by a well-defined central anomaly that has amplitudes ranging from 375 to 520 nT

and width ranging from 25 to 40 km. Magnetic lineations of anomalies J, 2 and 2A are identified on the both sides of the ridge axis. Seafloor spreading model studies indicate half spreading rates of 15.5 mm/yr on the south western flank and 13.4 mm/yr on the north eastern flank in this segment. Asymmetry in spreading indicated by the difference in half spreading rate is high in Segment I and Segment IV. Segment I and III displayed higher spreading rates on north-eastern side while in Segment IV the spreading rate is higher on the south-western side.

To obtain source magnetization, we carried out three-dimensional inversion of the magnetic data using the Fourier transform method (Parker and Huestis, 1974; Macdonald et al., 1980). The multibeam bathymetry at a grid spacing of 980 m was used for the inversion assuming a constant 500 m thickness for the source layer. Taylor expansion up to fifth order was carried out, 5 iterations brought sufficient convergence. The resultant magnetization solution (Figure 7) shows well defined magnetization stripes corresponding to the normal and reversely magnetized crust. Since we assumed constant thickness of magnetized layer in the inversion, regions of higher magnetization in the solution may also represent thickening of the source layer.

Central Indian Ridge

With few exceptions, the anomalies are well defined and correlatable. The amplitude of the central anomalies varied from 200 to 400 nT with about 100 nT local highs and lows in the middle, corresponding to the neo volcanic zone along the rift valley floor. These signature changes are probably the reflection of the magnetization variations within the crust. Magnetic anomalies up to 2A have been identified throughout the ridge section and anomaly 3 was seen along the profiles crossing segments N and O. The identified magnetic anomalies depict good agreement with the bathymetric lineation pattern and rift valley configuration. The asymmetry observed in the spreading rate is discernable on the topographic fabric and is prominent along the ridge segments bounded by the NTDs. Oblique bathymetric lineations are observed over the eastern flank of segment K1 around 5°S; however, the magnetic lineations corresponding to anomaly 2A in this region appear to be ridge parallel. The off axis trace of the NTD is seen extending till anomaly 2A suggesting that the NTD has existed since anomaly 2A time. However, the off-axis trace of the NTD between the segments M1 and M2 around 7°30'S is not significant. While the axial geometry is related to the local magma supply variations, there is no apparent correlation between the along axis depth variations and the inferred spreading rates. The finer variations observed in the spreading rates are attributed to local changes.

The inferred full spreading rates from the seafloor spreading models varied from 26 to 38 mm/yr. The spreading rates derived from the MORVEL model (DeMets et al., 2010) varied from 32 to 35 mm/yr and are comparable to the measured rates obtained from seafloor spreading model studies using the marine magnetic data. The rates derived from the MORVEL model increase linearly as the distance from the pole to the observational point increases. However, the measured full rates do not show systematic linear increase but vary from segment to segment.

Free-air and Mantle Bouguer gravity anomalies

a. Carlsberg Ridge

The free-air gravity anomalies over the CR varied from +45 to -60 mGals and typically mimicked the seafloor topography (Figure 8a). Prominent free-air gravity low all along the rift valley is conspicuous. The off-axis lows and highs corresponded to the ridge parallel topographic highs and lows and represented the anomalies arising from older seafloor. We have computed the MBA using the gridded values of topography and free-air anomaly in order to infer the subsurface mantle dynamics beneath the ridge segments. The MBA is computed by subtracting predictable effects of seafloor topography and the effect of crust/mantle interface from the free-air anomaly, assuming a constant 6.0 km thick oceanic crust, following the method described by Kuo and Forsyth (1988). Densities of 1.03, 2.73 and 3.33 g/cc were assumed for sea water, crust and mantle. The MBA map (Figure 8b) highlights the variations in the mantle and the deviations from the assumed thickness of the crust and serve as window to the mantle dynamics. MBA lows typically suggest thicker crust and usually observed at the segment centers of the ridge (Lin et al., 1990). The MBA highs observed near the segments ends and near to the transform fault regions suggest thin crust.

Two prominent MBA lows were observed over the CR around 04°05'N and 62°55'E longitude (B1); and 03°05'N latitude and 64°55'E longitude (B2) (Figure 8b). The B1 is observed over the linear segment with ridge parallel topographic fabric suggesting accretionary phase of evolution. Here the MBA low is elongated and it is about -30 mGal. The MBA low B2 is in the region of a shallow rift valley and the morphological characters suggest dominance of magmatic process. The circular MBA low of -50 mGal observed here is inferred to be due to the mantle upwelling leading to the thickening of the crust.

Central Indian Ridge

The free-air gravity anomalies over the CIR have followed the topography; the rift valley and the prominent bathymetric low observed over the Vema transform fault

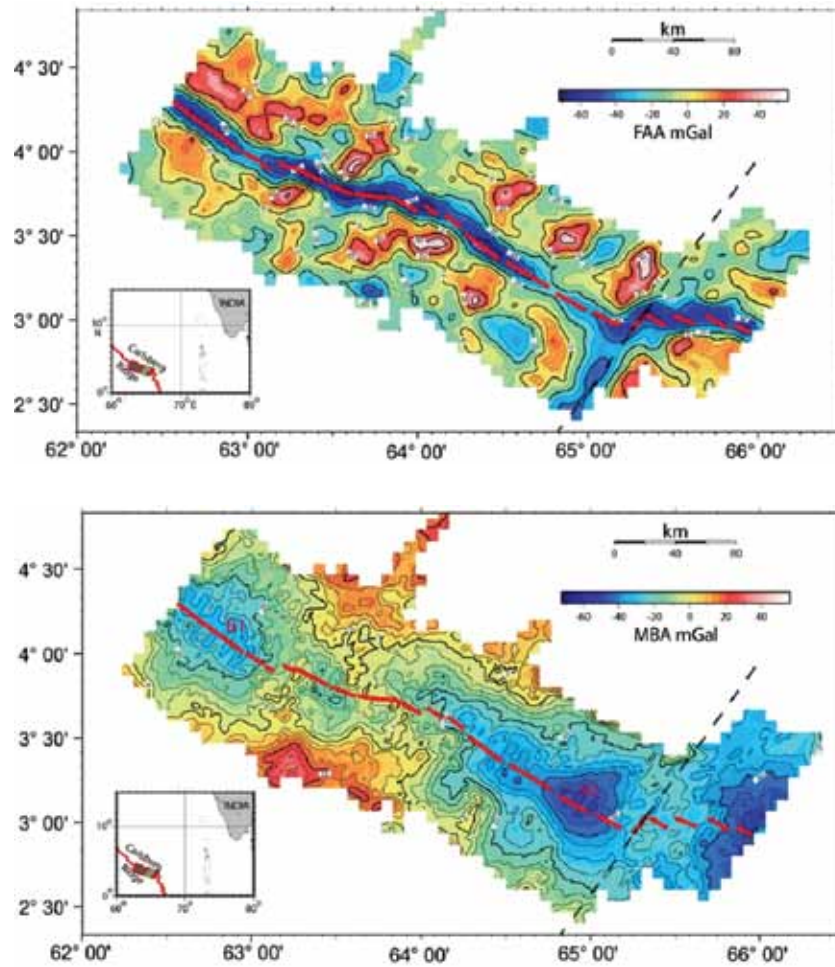


Figure 8. a. Free-air anomaly and b. Mantle Bouguer anomaly maps of a part of the Carlsberg Ridge. Thick red line indicates the ridge axis. B1 and B2 represent prominent MBA lows.

are characterized by the significant free-air gravity lows. Here we present topography, free-air gravity and mantle Bouguer anomalies (Figure 9) over linear segment of the CIR corresponding to the segment L (Figure 4) of the ridge. The free-air gravity approximates the topography (Figure 9a) reflecting major features observed on the bathymetric map. The rift valley shallows toward NW side, defined by a FAA low of about -10 to -80 mGals, the lowest being at the ridge-transform intersection (Figure 9b). In order to visualize the sub-seafloor density structure we computed mantle Bouguer anomaly (MBA). The MBA map contoured at 5 mGals interval (Figure 9c) depicts a lowest value of -55 mGals in the NW part of the segment where the median valley shallows. The circular MBA observed here is similar to the 'bull's eye' MBA low observed over Mid-Atlantic ridge segments (Lin et al. 1990; Lin and Morgan 1992; Tolstoy et al. 1993). These were interpreted in terms of focused magmatic accretion resulting in significant crustal thickness variations over the ridge segments. In the present study the along axis variations of depth, free-air gravity and

MBA show shallowing of the spreading axis in the middle of the ridge segment with an MBA low of -55 mGals. The MBA low observed here indicates along axis thickness variations in crust. The well developed rift valley and the observed relative MBA highs towards SE (Figure 9c) suggest depleted accretion and crustal thinning at the transforms and at the RTI high. The increase in MBA away from the ridge axis and at the transforms were predicted along the Mid-Atlantic ridge segments (Neumann and Forsyth 1993) using isoviscous, passive, flat plate model of Phipps Morgan and Forsyth (1988).

SEABED SAMPLING

Petrography of the Carlsberg Ridge and Central Indian Ridge

The first report of basalts from Carlsberg Ridge was by Wiseman & Poole (1937) collected at 01°25'12"S and 66°34'12"E, during Mahahiss cruise from Zanzibar to

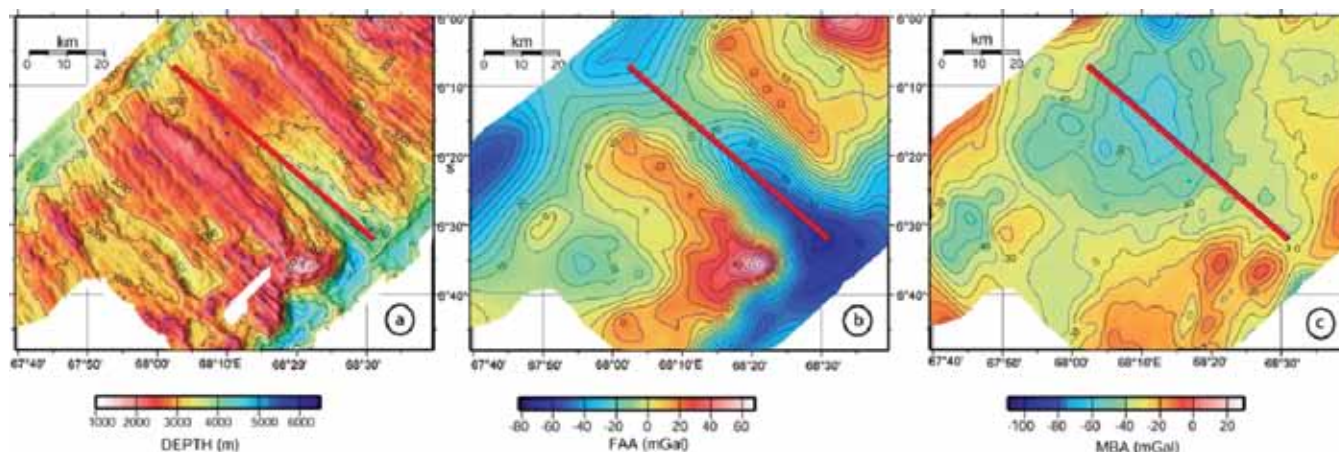


Figure 9. a. Topography, b. free-air gravity and c. mantle Bouguer anomaly (MBA) maps of a linear segment of the Central Indian Ridge.

Colombo. Different types of basalts identified in this expedition were augite basalt, variolitic basalt (based on the micro-texture); hornblende-augite-dolerite, based on the mineralogy and major element composition. The rocks were comparable to the rocks recovered from Atlantic and Pacific oceans. The initiation of Indian Ridge program has seen marked improvement in the coverage of samples along the CR and CIR. Sampling along the axial region of the CR and CIR has been carried out based on multibeam maps (Mudholkar et al., 2002; Kamesh Raju et al., 2008, Kamesh Raju et al., 2012).

Seabed sampling along the ridge recovered mostly fresh basalts along the rift valley floor and flanks, mantle rocks were recovered at three RTI highs. Mantle derived rocks such as peridotites and serpentinites were found at two locations (Figure 3) (Mudholkar et al., 2002; Kamesh Raju et al., 2008) along the CR. Fresh basalts and serpentinitized peridotites were recovered over the megamullion structures over the Central Indian Ridge segments (Ray et al., 2013). Presence of serpentinites at the megamullion structure M1 (Figure 4) indicates mantle derived material. The exposure of peridotites indicative of upper mantle rocks implies thin crust and moderate supply of magma.

Ultramafic rocks

Along the mid-ocean ridges, the mantle rocks represented by serpentinites and peridotites which are composed of ferromagnesian minerals such as olivine altered to serpentine, pyroxenes and diverse spinels, are exposed mostly on the ridge flanks and/or on the inside of the ridge wall. Ultramafic rocks get exposed due to the tectonic uplifting and also due to the volume expansion by hydration of the serpentine-rich rocks. Earlier these mantle rocks were considered to have been uplifted due to tectonic forces (Bonatti 1978; Bonatti and Hamlyn, 1978). Better

mapping and sampling over the ridges lead Tucholke et al. (1998) to propose that the detachment fault tectonics play an important role in the emplacement of the lower crustal gabbros and upper mantle peridotite and serpentinite rocks on the ocean floor.

The ultramafic rocks of the CR are dominated by serpentinites followed by spinel lherzolites with varying degrees of serpentinization. Mineralogically, lherzolite is composed of forsterite (Mg-rich olivine altered to serpentine), enstatite (CPx), diopside (CPx) and accessory spinel. Although the lherzolites are serpentinized with hour glass textures, fresh bastite textures and sufficient modal proportion of anhydrous silicates are preserved from which it is easy to decipher the original textures. Serpentinized ultramafics or mixture of basalts and ultramafic outcrops are commonly found at active hydrothermal fields over the slow spreading MAR (Rona et al., 1987; Bougault et al., 1993; Gracia et al., 2000; Da Costa et al., 2008; Marbler et al., 2010), CIR (Morishita et al., 2009), and ultra-slow Southwest Indian Ridge (Bach et al., 2002) and Mid-Cayman Rise (German et al., 2010).

Gabbros

Few pieces of gabbros were recovered from the narrow axial valley high near the RAD of the Carlsberg Ridge (Figure 3) along with the serpentinites and peridotites. The gabbros are fresh and show little alteration due to seawater. These are coarsely crystalline rocks with large crystals of ferromagnesian minerals as well as feldspars can be seen in hand specimen.

The principal mineral components of the recovered gabbros are orthopyroxenes, feldspars and spinels. These gabbros do not contain olivine and are therefore termed as norite type. The feldspars are mostly calcic (anorthitic) though sodic (orthoclase type) feldspars are present and they

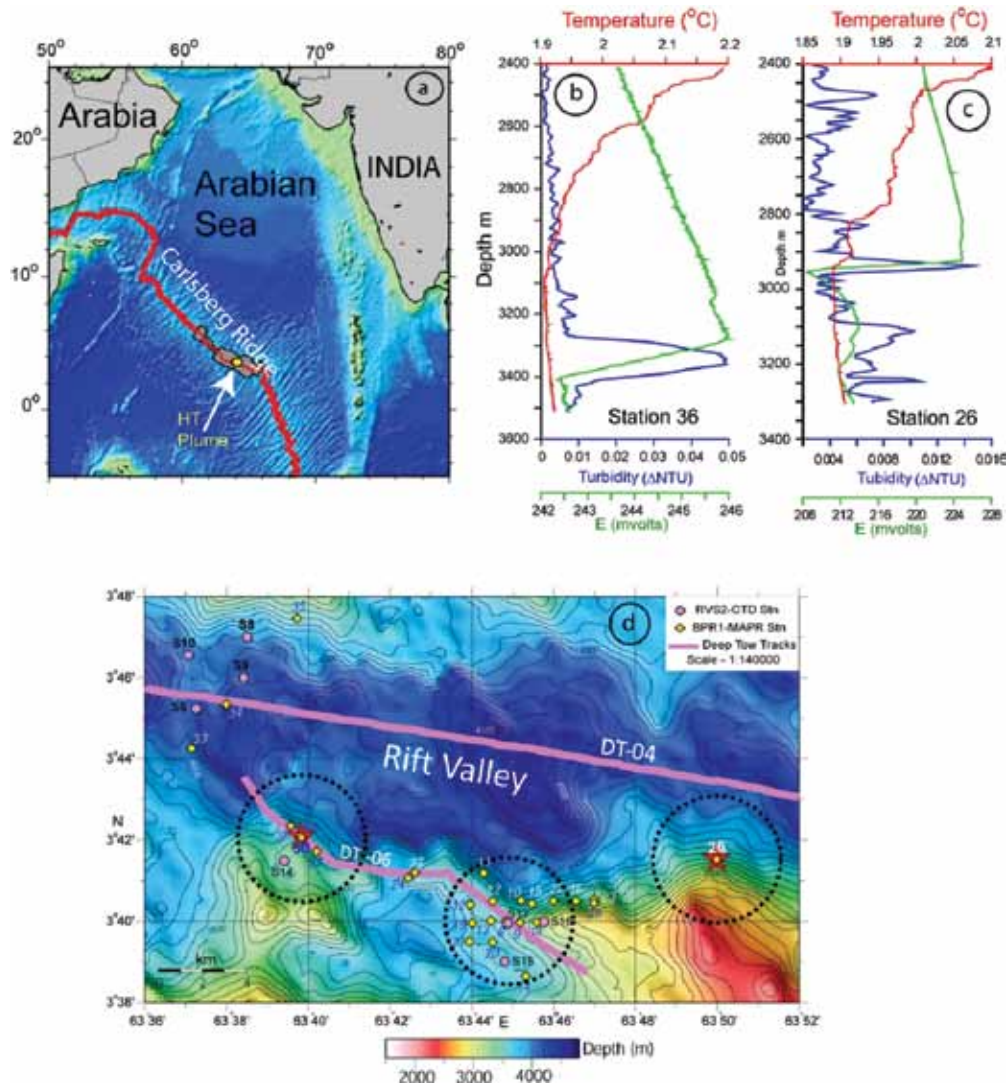


Figure 10. Active unconfirmed vent fields over the Carlsberg Ridge. a. Plume location based on chemical and optical signatures in the water column. b & c temperature, turbidity and oxidation reduction potential (ORP) signatures (E) in the water column at stations 36 and 26 respectively. d. detailed bathymetry of the plume region along with spreading center, deep-tow tracks, CTD and MAPR cast locations.

exhibit cross hatching pattern. The plagioclase feldspars are of bytownite to labradorite composition with Ab content ~ 34-48. Diopsidic augite grains are few in gabbro and they do not form a major mineral component. Orthopyroxenes are more in modal percentage (~40-45%) while clinopyroxenes are less (~5-8%). The altered amphiboles also exhibit pleochroism in shades of green and brown. Many orthopyroxene crystals exhibit total alteration to green coloured urallite with a fibrous texture. Granulation along few crystal boundaries is seen indicating that these gabbros have undergone the cataclysmic metamorphism. This inter-crystal granulation might have been caused due to the tectonic movements along the ridge axis which may be a post-emplacement process.

HYDROTHERMAL VENT EXPLORATION

Active vents continuously emit hydrothermal fluids of magmatic origin, these are well known along the world mid-ocean ridge system (Figure 1) and are indicative of hydrothermal vent fields. Large-scale, systematic searches have discovered active vent fields with increasing frequency since the early 1990s (Baker and German, 2004). Based on optical backscatter, light transmission and chemical tracers in water column, existence of neutrally buoyant plumes have been inferred at few locations on Southeast Indian ridge, CIR, CR, and Gulf of Aden (Jean-Baptiste et al., 1992; German et al., 1998; Scheirer et al. 1998; Gamo et al., 2001; Bach et al. 2002; Ray et al 2012, Tao et. al., 2012, Son et al., 2014).

Hydrothermal plumes over the Carlsberg ridge

An unusually large event plume “CR2003” was reported over the CR (Murton et al. 2006). In terms of heat generation ($74\text{-}240 \times 10^{15}$ Joule), plume raising height (1400 m from seafloor), plume width (>70 km), the CR2003 event was largest among the plume recorded till date in the world oceans. Subsequent observations by Ray et al. 2008 reported reduced intensity of the plume within water column between 2500 and 2900 m. The maxima of dissolved manganese of ~ 15 nmol/l at 2500 m were decreased to ~ 12 nmol/l at 2700 m. Further an additional plume layer at water depth > 3100 m around the same location has been inferred as deeper plume and could be due to a successive hydrothermal event (Ray et al., 2008).

Besides the event plume, chronic hydrothermal plumes from unknown active vents have been discovered over this slow-spreading Carlsberg Ridge in the northern Indian Ocean (Ray et al 2012). A continuous deep-tow all along the 440 km rift valley zone of the CR in December 2007 using IMI-30 Deep tow system and Miniature Autonomous Plume Recorders (MAPRs) onboard RV Sonne, resulted in scanning the waters for plume signatures. Following the deep tow-MAPR survey, several CTD hydrocasts have been used to collect precise hydrographic data and water samples. The plume was identified in water column between 2950 and 3200m near $03^{\circ}40'N$, $63^{\circ}45'E$, based on physiochemical signatures like potential temperature, optical backscatter (OBS), dissolved manganese (DMn) and helium.

A second expedition to the same region, undertaken in April-May 2009 onboard RV *Akademik Boris Petrov* (BPR-1 cruise) conducted 23 MAPR hydrocasts around the location where plume signatures were first observed in 2007. MAPRs were equipped with high-precision temperature sensors, light back-scattering sensors, and oxidation-reduction potential (ORP) sensors. ORP values (E in mvolts) are highly sensitive to short-lived reduced chemicals in hydrothermal plumes, such as Fe^{2+} and H_2S , and generally occur as a sharp decline in E followed by a gradual recovery (Nakamura et al., 2000; Walker et al., 2007). Depending on local current speed, significant E drops are only observed within a radius of ~ 1.0 km of an active hydrothermal source (Walker et al., 2007; German et al., 2008), and so are especially valuable in determining source location. During this investigation two non-buoyant plumes were found at the depths of about 2900 and 3200 m near $03^{\circ}42'N$, $63^{\circ}40'E$ and $03^{\circ}41.5'N$, $63^{\circ}50'E$ respectively. Both the plumes were characterized with prominent backscatter ($\Delta NTU \sim 0.015$ to 0.05) and ORP anomalies (max. $\Delta E \sim 17$ mvolts).

Based on the character of the plume signatures it was concluded that these plumes are emanating from two independent vent fields (Figure 10) in the vicinity (Ray et

al., 2012). Ultramafic rocks have been recovered at few dredging stations in this area consisting of peridotite, serpentinite, gabbro and basalts. The dissolved Mn anomalies and significant reducing conditions in the deep water column imply that the plumes arise from both ultramafic and basaltic/gabbroic fluid-rock interaction. It is inferred that the nature of plumes are very similar to that found in Rainbow and Logatchev fields of the MAR (Ray et al., 2012). A more precise AUV survey to pin point the source location and an ROV survey to image and sample the vents is required.

Newly discovered hydrothermal activity over the CIR based on AUV investigations

During a cruise onboard ORV Sagar Nidhi, a 30 mile segment near $10^{\circ}S$ of CIR has been explored for seafloor hydrothermal activity. During this expedition we have discovered a hydrothermal plume over an hitherto unexplored segment of the Central Indian Ridge south of $10^{\circ}S$ in about 10 days ship time. This discovery has been possible due to the use of multi-parameter and multi-platform (Shipboard and AUV) exploration strategy (CSIR-NIO-cruise report-SN48).

Based on CTD and MAPR observations we selected an area for AUV (ABYSS from IFM-GEOMER) survey near the western wall of the rift valley. Abyss equipped with multi-beam, CTD, backscatter and redox (Eh) sensors was deployed to investigate the water column at 3200 m as well as to map the seafloor. Results show increase of *in situ* temperature and drops in Eh in water layer away from the valley wall. Chemical analysis of seawater collected from the turbid layer show higher level dissolved manganese (~ 20 nmol/l). Our results, particularly, optical backscatter and dissolved manganese signatures in water column indicate the possibility of hydrothermal emission from unknown active source(s). A more detailed investigation is required to confirm the new active hydrothermal field(s) around this area. This expedition has demonstrated the effectiveness of using modern vessel with precise navigation and station keeping capabilities (with dynamic positioning) and use of AUV by locating hydrothermal plumes in limited ship-time. Further, the first systematic surveys using a combination of CTD-MAPR-Seabed sampling between $8^{\circ}S$ and $17^{\circ}S$ over the CIR by Son et al., (2014), provided evidence for extensive hydrothermal plumes in the water column above the rift valley.

DISCUSSION

Segmentation vs. spreading rate

Significantly different ridge segmentation patterns have been observed on both Carlsberg and Central Indian ridges.

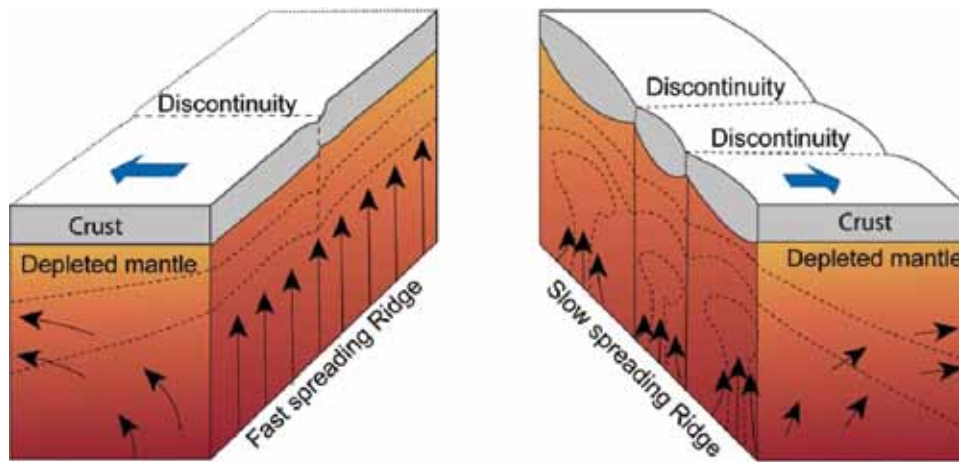


Figure 11. Schematic representation of spreading rate dependant model of crustal accretion and mantle upwelling beneath the fast and slow spreading ridges derived from bathymetry and gravity observations (after Lin and Morgan, 1990). Dashed lines represent the isotherms; thin arrows in the mantle indicate dominant direction of flow. The blue arrows represent the direction of plate motion. Note the distinctly different crustal structure and segmentation arising from uniform and discrete spreading cells in response to fast and slow spreading ridge systems respectively.

Both these ridges fall under the ‘slow-spreading’ M-O-R classification (Dick et al., 2003). The CR and CIR belong to the slow spreading ridges with 22-40 mm/yr spreading rate (Kamesh Raju et al., 2008; 2012; Son et al., 2014), the SWIR is a very-slow spreading system with spreading rates in the range of 12-16 mm/yr (German et al., 1998) and the SEIR is an intermediate spreading center with spreading rates varying from 59 to 75 mm/yr (Cochran et al., 1997; Small et al., 1999). We would like to place the Southwest Indian ridge (SWIR) as a very slow spreading class of ridge due its distinctly contrasting nature compared to other slow spreading ridges such as Mid-Atlantic Ridge (MAR), CR and the CIR. While defining the ultraslow spreading (8-13 mm/yr) Gakkel ridge, Dick et al. (2003) suggested that the very slow spreading (12-16 mm/yr) SWIR and the arctic ridges spreading at 13-18 mm/yr are transitional between slow and ultraslow spreading ridges. We concur with the view that these ridges display slow or ultra slow morphology over long sections (Dick et al., 2003). Among the Indian Ocean ridge systems the SWIR and parts of the SEIR are better explored than the CR and CIR. The CR exhibited a long section of the ridge without major transforms, much like the section of MAR between Kane and Atlantis transforms (Sempere et al., 1990; Gente, et al., 1995), where as the CIR has systematic segmentation pattern bordered by well defined transform faults. The CR at 22 - 32 mm spread rate is spreading at a lower rate than the CIR that spreads at 26 - 40 mm per year. The spreading rate dependency on the segmentation patters have been studied (Lin and Morgan, 1992; Bohnenstiehl and Kleinrock, 2000) and in general it has been observed that the slow spreading ridges have short segments with

well defined TFs and the very-slow spreading ridges like SWIR are characterized with shorter segments. On the other hand fast spreading ridges like EPR (Macdonald et al. 1991) are characterized by long uninterrupted segments. The fast spreading ridges are supported by robust magma supply, well defined magma chambers have been imaged beneath these segments (Detrick et al., 1987; Carbotte et al., 2012). Recent analysis of 2D and 3D Seismic data over EPR suggests that vertical ascent of magma lenses induce fine-scale tectonic segmentation observed at fast spreading ridges (Carbotte et al., 2013). Whereas the slow spreading ridges are supported by smaller magma cells, these magma upwelling centers have been indicated by typical ‘bull’s eye’ mantle Bouguer anomaly lows (Lin et al., 1990). Gravity data analysis (Lin and Morgan, 1992) have shown that the crustal density structure is relatively uniform at the fast spreading ridges such as EPR compared to the slow spreading MAR. Plume-like mantle upwelling and melting beneath the slow spreading ridges results in continuously varying crustal thickness, whereas a relatively uniform thick crust over the fast spreading ridges is attributed to the sheet-like mantle upwelling (Lin et al., 1990; Lin and Morgan, 1992) over the fast spreading ridges (Figure 11). However, we do not know, how the finer scale spreading rate differences effect the ridge segmentation pattern. It has been observed elsewhere and also in the present study that slow spreading ridges exhibit fast spreading morphologies at isolated segments, some of these are explained by the ridge-hot spot interactions (Dyment et al., 2007); however there are some long sections where there is no hot spot influence, for e.g., section of MAR between 24°-30°N, Kane and Atlantis transforms. The existence of long ridge

segments over the slow spreading ridges appears to be an exception and is at variance to the widely observed general segmentation pattern of the slow spreading ridges. Ridge propagation and the existence of new class of offsets called the non-transform offsets could be the possible mechanisms that sustain long sections of the slow-spreading ridges without a first order segmentation. The long section of the Carlsberg Ridge between 58° – 65°E is one such example of a long ridge segment without major transforms over a slow spreading ridge.

Mantle Signatures

The occurrence of focused magma upwelling zones as indicated by the MBA lows, greatly influence the topographic character of the ridge segments. Combination of the magmatic and less magmatic processes results in ridge segments that are highly variable in terms of rift valley morphology and the ridge flank topographic fabric. Such characterization is discernable on the surveyed sections of the CR and CIR (Kamesh Raju et al., 2008; Kamesh Raju et al., 2012, Son et al., 2014). The manifestation of the effect of magma supply over the rift valley morphology is conspicuous on the slow spreading ridges that are supported by discrete cells of focused magma supply zones, in contrast to uniform crustal thickness (Lin and Morgan, 1992; Tolstoy et al., 1993) over the fast spreading ridges. It is also observed that magmatic segments are associated with well defined transform faults while the less magmatic sections are often associated with NTDs. The NTDs are non-steady state features that are spatially and temporally variable (Macdonald et al., 1988) and respond to changes in melt driven processes. The magmatic influx of both the segments of the NTD is independently modulated and results in the lengthening of the more magmatic segment at the expense of the less magmatic segment (Gac et al., 2006).

The exposures of ultramafic rocks at the segment ends and at the NTD's also support the thin crust at these locations. Of particular interest are the core complexes or the megamullion structures observed at the ridge transform intersections and at the inside corners. Megamullions are large (up to 10's of km on a side) domed seafloor edifices that have surfaces corrugated by distinctive mullion structure and that normally are developed at the inside-corner tectonic settings at the ends of spreading segments. Their characteristic structure, together with recovery of gabbros, serpentinized peridotites, and fault rocks (e.g., mylonites) at or near their surfaces, indicate that they are formed by long-lived (~1-2 m.y.) normal, 'detachment' faults and that they expose 'core complexes' of exhumed lower-crustal to upper-mantle rocks. Most megamullions are associated with elevated gravity anomalies and they are typically 10-20 mGal more positive than over the surrounding crust, equivalent to relative crustal thinning

of at least 1-2 km (Blackman et al., 2009). These features, and the fact that megamullions tend to form at segment ends where melt supply is lower than at the segment centers, indicate that they form during periods of reduced magmatism compared to normal spreading (Escartin and Lin, 1995; Escartin et al., 2008; Tucholke et al., 1998, 2008). On the other hand, if detachment faulting were enhanced with increased tectonic extension, megamullions should be abundant on slower-spreading ridges, but their frequency there is limited. For example, they cover only 4% of the seafloor on the ultraslow Southwest Indian Ridge (Cannat et al., 2006), and none have been identified on Gakkel Ridge, the slowest-spreading MOR on Earth (Dick et al., 2003; Michael et al., 2003). Tucholke et al., 2008, used numerical models and analysed geological data for megamullions to assess the role of magmatism in normal faulting and concluded that continuous detachment faults develop at intermediate levels of magma supply. These studies have also suggested that large-scale corrugations on detachments are linked to brittle-plastic transition above magmatic intrusions, implying that magmatism is an integral part of megamullion formation.

Three well defined OCC/megamullion structures have been identified on CIR (Kamesh Raju et al., 2012). The megamullion structures provide an excellent opportunity to study the mantle heterogeneities by carrying out OBS seismic experiments and by detailed sampling using TV-linked grabs and submersibles, and by conducting deep drilling studies. Two megamullion structures on the MAR and one on the Southwest Indian Ridge have been drilled by ODP, and in each case thick (up to 1.4 km) gabbros were cored, indicating a strong magmatic component (Dick et al., 2000; Kelemen et al., 2004; Blackman et al., 2006).

Vent fields

The Sheba, Carlsberg and Central Indian ridges bisect the Indian Ocean from the Rodriguez Triple Junction at 25°S to the entrance of the Gulf of Aden at 15°N. Hydrothermal exploration has been sparse along this lengthy section of slow-spreading ridge consisting of Carlsberg and the Central Indian Ridges. Most of the early investigations concentrated at ridge segments south of ~18°S (Gamo et al., 1996, 2001; Van Dover et al., 2001; Kawagucci et al., 2008) and near to the Indian Ocean Triple Junction (Honsho et al., 1996; Sauter et al., 1996; Mendel et al., 2000; Hashimoto et al., 2001; Van Dover et al., 2001; Tamaki et al., 2010). Murton et al. (2006) reported evidence of an event plume between 5°41'N and 6°20'N, their data was insufficient to locate the seafloor source of the plume. Subsequent detailed investigations between 62°-66° E longitudes using deep-tow, CTD, MAPR casts and TV-grab onboard RV Sonne in 2005 and repeat survey by RV Boris Petrov, provided evidence

for two vent fields, one near 3°42'N, 63°40'E and another near 3°41.5'N, 63°50'E over the CR (Ray et al., 2012) and also at 3°39.5'N, 63°45.5'E (Figure 9).

Extensive hydrothermal plumes have been reported from the CIR between 8°S and 17°S (Son et al., 2014). Exploration north of the Rodriguez Triple Junction has led to the discovery of two active vents: the Kairei field at 25°19.2'S, 70°2.4'E (Hashimoto et al., 2001; Gamo et al., 2001; Van Dover et al., 2001), and the Edmond field at 23°52.7'S, 69°35.8'E (Van Dover et al., 2001). Nearly after a decade the Japanese group has discovered two more active hydrothermal sites at 18°20'S and at 19°33'S latitudes over the CIR. These fields are named as Dodo and Solitaire respectively. Manned deep-sea submersible vehicle (DSV) Shikai6500 was deployed for this discovery (Tamaki et al., 2010).

The largest sulphide deposits are found on slow spreading ridges where volcanism is episodic and alternates with long periods of intense tectonic activity with few eruptions (Fouquet, 1997; Hannington et al., 2005). The studies carried out over the slow spreading ridges have increasingly shown that these are better targets for long lived hydrothermal systems as they have less frequent eruptions, lower rate of magma supply and greater structural control, factors that facilitate hydrothermal fluid up-flow and circulation (Singh et al., 2006). As a consequence, the slow spreading ridge segments are more sought after locations for massive sulphide deposits and mineral resources (Hannington et al., 1998; Rona, 2003, Rona, 2008). The TAG HT field is the most well studied system on the slow spreading MAR, where a series of holes drilled under the ODP leg 157 have provided insights into the workings of an active HT field (Humphris et al., 1995). Surveys of the Gakkel and Knipovich Ridges found even more stunning hydrothermal evidence, with multiple active sites inferred from plume observations (Edmonds et al., 2001; German et al., 2010; Connelly et al., 2010). Furthermore, recent discoveries of sulphide deposits from ultra-slow spreading ridges (Baker et al., 2004; Münch et al., 2001; Snow et al., 2001; Edmonds et al., 2001) suggest that massive sulphide formation can also take place at ridges with extremely low magma budgets.

Recent review of active vent fields in the world oceans and the associated probable sulfide mineral resources (Hannington et al., 2011), have concluded that the slow spreading ridges are the most promising regions for long-lived hydrothermal venting and thereby are the potential targets for hydrothermal sulfide mineral resources. Considering various parameters the study estimates a vent source for every 150 km along axis distance of a slow spreading ridge. Therefore, the Indian Ocean ridges provide a great opportunity for discovering new active hydrothermal vent fields that support unique seafloor and subsea-floor deep-sea ecosystems and hold promise of mineral resources.

CONCLUSIONS

The CR and CIR ridge sections have distinctly different partitioning in terms of first order discontinuities, even though they belong to the slow-spreading class of the MORs. While CR has displayed transform faults at regular intervals the CR has a long section dominated by NTDs. NTDs are probably the mechanism that sustain long segments of the CR. Combinations of magmatic and less magmatic segments characterize both CR and CIR ridge sections. It is observed that magmatic segments are associated with well defined transform faults while the less magmatic sections are often associated with NTDs.

The MBA gravity signatures on CR and CIR reflect focused mantle upwelling zones along these slow spreading ridges. The MBA low observed over the CR is more prominent with a near circular -50 mGal low. The shallowing of rift valley and the propagating ridge feature observed at this location suggests crustal thickening. The magnetic inversion studies indicated pockets of high magnetization zones along the rift valley floor of the CR, these highs correspond to the neo-volcanic zones manifested as axial volcanic ridges.

Prominent megamullion/OCC structures have been documented at the inside corner settings of CIR, these are located at the less magmatic segments of the ridge. No prominent megamullion structure has been identified over the section of the CR, however, mantle rock exposures have been noticed at the non-transform discontinuities and also at the amagmatic segments.

Two prominent new vent fields over CR and possible plume signatures over the CIR have been identified as a result of detailed investigations over CR and CIR. These vent fields and plume signatures are identified based on the optical and chemical signatures observed in the water column and therefore are classified as active unconfirmed vents. AUV and ROV investigations are required to confirm and sample these hydrothermal vents.

Considering the tectonic and magmatic characteristics and the recent global estimates of the frequency of the vent fields over the slow spreading ridges, we can expect that the global average of a vent field for every 150-200 km along axis distance of the ridge may hold good for CR and CIR sections of the slow spreading ridge system. With limited number of confirmed active vents, the slow spreading Indian Ocean ridges (CR and CIR) provide excellent opportunity for discovering new active hydrothermal vent fields that hold promise of mineral resources and support unique seafloor and subsea-floor deep-sea ecosystems.

ACKNOWLEDGEMENTS

We thank Dr. S.W.A. Naqvi, Director, CSIR-National Institute of Oceanography, Goa, for the encouragement

and support given to carry out this study. Our sincere thanks to all the ridge team members and colleagues contributed in acquiring quality data and participated in fruitful discussions. We are thankful to Dr. P.R. Reddy, Editor of the Journal for providing valuable suggestions for the refinement of the manuscript. The ridge program is funded by the CSIR under the Network program and the Ministry of Earth Sciences (MoES) under the Hydrothermal Sulphides program. Our sincere thanks are due to the funding agencies. This is CSIR-N.I.O. contribution.

REFERENCES

- Bach, W., Banerjee, N.R., Dick, H.J.B., and Baker, E.T., 2002. Discovery of ancient and active hydrothermal systems along the ultra-slow spreading Southwest Indian Ridge 10° – 16°E, *Geochem. Geophys. Geosyst.*, 3, doi: 10.1029/2001GC000279.
- Baker E.T., and German C.R., 2004. On the global distribution of hydrothermal vent fields. In: *Mid-Ocean Ridges: Hydrothermal Interactions Between the Lithosphere and Oceans*, Geophysical Monograph Series 148, German, C.R., Lin, J., and Parson, L.M., (eds.), published by the American Geophysical Union. pp: 245–266.
- Baker, E. T., Edmonds, H. N., Michael, P. J., Bach, W., Dick, H.J.B., Snow, J.E., Walker, S. L., Banerjee, N. R., and Langmuir, C.H., 2004. Hydrothermal venting in magma deserts: The ultraslow-spreading Gakkel and Southwest Indian Ridges, *Geochem. Geophys. Geosyst.*, 5, Q08002, doi:10.1029/2004GC000712
- Beaulieu, S.E., 2010. InterRidge Global Database of Active Submarine Hydrothermal Vent Fields: prepared for InterRidge, Version 2.0. World Wide Web electronic publication. <http://www.interridge.org/IRvents>
- Beaulieu, S.E., Baker, E.T., German, C.R., Maffei, A., 2013. An authoritative global database for active submarine hydrothermal vent fields. *Geochem. Geophys. Geosyst.*, v.14, pp:4892-4905, doi:10.1002/2013GC004998.
- Blackman, D. K., Ildefonse, B., John, B. E., Ohara, Y., Miller, D. J., MacLeod, C. J., and the Expedition 304/305 Scientists, 2006. *Proc. IODP*, 304/305: Washington, DC (Integrated Ocean Drilling Program Management International, Inc.). doi:10.2204/iodp.proc.304305.2006.
- Blackman, D.K., Cannales, J.P., Harding, A., 2009. Geophysical signatures of oceanic core complexes. *Geophys. J. Int.*, v.178, pp: 593-613.
- Bohnenstiehl, R. D., and Kleinrock, M.C., 2000. Evidence for spreading rate dependence in the displacement – length ratio of abyssal hill faults at mid-ocean ridges, *Geology*, v. 28, pp: 395-398.
- Bonatti, E., 1978. Vertical tectonism in oceanic fracture zones. *Earth Planet. Sci. Lett.*, v. 37 pp: 369-379.
- Bonatti, E., and Hamlyn, P.R., 1978. Mantle uplifted block in the western Indian Ocean. *Science*, v.201, pp: 249-251.
- Bougault, H., J. L. Charlou, Y. Fouquet, H. D. Needham, N. Vaslet, P., Appriou, P. Jean-Baptiste, P. A. Rona, L. Dmitriev, and S. Silantiev (1993), Fast and slow spreading ridges: structures and hydrothermal activity, ultramafic topographic highs, and CH₄ output, *J. Geophys. Res.*, v.98, pp:9643-9651.
- Briais, A., 1995. Structural analysis of the segmentation of the Central Indian Ridge between 20°30' and 25°30' S (Rodriguez Triple Junction), *Mar. Geophys. Res.*, v.17, pp: 431–467.
- Cannat, M., Mevel, C., Maia, M., Deplus, C., Gente, P., Agrinier, P., Belarouchi, A., Dubuisson, G., Humler, E., Reynolds, J., 1995. Thin crust, ultramafic exposures, and rugged faulting patterns at the Mid-Atlantic Ridge (22°-24°N), *Geology*, v. 23, pp:49-52.
- Cannat, M., Lagabriele, Y., Bougault, H., Casey, J., Nathalie de Coutures, Dmitriev, L., Fouquet, Y., 1997. Ultramafic and gabbroic exposures at the Mid-Atlantic Ridge: geological mapping in the 15°N region, *Tectonophysics*, v. 279, pp: 193-213.
- Cannat, M., Sauter, D., Mendel, V., Ruellan, E., Okhino, K., Escartin, J., Combiér, V., and Baala, M., 2006. Modes of seafloor generation at a melt-poor ultraslow-spreading ridge, *Geology*, v.34, pp: 605-608, doi:10.1130/G22486.1.
- Cande S.C., Kent D.V., 1995. Revised calibration of the geomagnetic polarity timescale for the late Cretaceous and Cenozoic, *J. Geophys. Res.* v.100, pp: 6093-6095.
- Carbotte, S.M., Canales, J.P., Nedimović, M.R., Carton, H., and Mutter, J.C., 2012. Recent seismic studies at the East Pacific Rise 8°20'–10°10'N and Endeavour Segment: Insights into mid-ocean ridge hydrothermal and magmatic processes, *Oceanography*, v.25, pp: 100–112.
- Caress, D.W., Chayes, D.N., 1995. MB-system, developed at Lamont-Doherty Earth Observatory report.
- Cochran, J. R., J. Sempe´re´, and SEIR Scientific Team, 1997. The Southeast Indian Ridge between 88°E and 118°E: Gravity anomalies and crustal accretion at intermediate spreading rates, *J. Geophys. Res.*, v.102, pp: 15463–15488.
- Cochran, J.R., Kurrus, G.J., Edwards, M.H., Coakley, B.J., 2003. The Gakkel Ridge: Bathymetry, gravity anomalies and crustal accretion at extremely slow spreading rates, *J. Geophys. Res.*, v.108, doi: 10/1029/2002JB001830.
- Connelly, D.P., and JC44 scientific party, 2010. New Hydrothermal Vents Located on the Mid-Cayman Spreading Centre: Cruise RRS James Cook 44, March-April 2010, *INTERRIDGE NEWS* 23., v.19, 2010.
- Corlisis, J.B., Dymond, J., Gordon, L.I., Edmond, J.M., Von Herzen, R., Ballard, R., Green, K., Williams, D., Bainbridge, A., Crane, K., van Andel, T.H., 1979. Submarine thermal springs on the Galapagos rift, *Science*, v.203, pp:1073-1083.
- DaCosta, I. R., F. J. A. S. Barriga, and R. N., Taylor, 2008. Late seafloor carbonate precipitation in serpentinites from the Rainbow and Saldanha sites (Mid-Atlantic Ridge), *Europe. J. Mineral.*, v.20, pp: 173-181.
- DeMets, C., Gordon, R. G., and Vogt, P., 1994. Location of

- the Africa-Australia-India triple junction and motion between the Australian and Indian plates: Results from an aeromagnetic investigation of the Central Indian and Carlsberg ridges, *Geophys. J. Int.*, v.119, pp: 893–930.
- DeMets, C., Gordon, R.G., Argus, D.F., 2010. Geologically current plate motions, *Geophys. J. Int.*, v.181, pp:1-80.
- Detrick, R. S. et al. Multi-channel seismic imaging of a crustal magma chamber along the East Pacific Rise, 1987. *Nature*, v.326, pp: 35–41.
- Dick, H.J.B., Natland, J.H., Alt, J.C., Bach, W., Bideau, D., Gee, J.S., Haggas, S., Hertogen, J.G.H., Hirth, G., Holm, P.M., Ildefonse, B., Iturrino, G.J., John, B.E., Kelley, D.S., Kikawa, E., Kingdon, A., LeRoux, P.J., Maeda, J., Meyer, P.S., Miller, D.J., Naslund, H.R., Niu, Y., Robinson, P.T., Snow, J., Stephen, R.A., Trimby, P.W., Worm, H.-U., and Yoshinobu, A., 2000. A long in situ section of the lower ocean crust: results of ODP Leg 176 drilling at the Southwest Indian Ridge. *Earth Planet. Sci. Lett.*, v.179, pp:31-51. doi:10.1016/S0012-821X(00)00102-3
- Dick, H.J.B., Lin, J., Schouten, H., 2003. An ultraslow- spreading class of Ocean ridge, *Nature* v.426, pp: 405-412.
- Drobia, R. K., Ghose, I., Subramanyam, A. S., Malleswara Rao, M. M., Kessarkar, P., and Murthy, K. S. R., 2000. Magnetic and bathymetric investigations over the Vema Region of the Central Indian Ridge: Tectonic implications, *Mar. Geol.*, v.167, pp: 413–423.
- Drobia, R. K., and DeMets, C., 2005. Deformation in the diffuse India-Capricorn-Somalia triple junction from a multibeam and magnetic survey of the northern Central Indian ridge 3°S–10°S, *Geochem. Geophys. Geosyst.*, 6, Q09009, doi: 10.1029/2005GC000950.
- Dyment, J., Lin, J., and Baker, E.T., 2007. Ridge-hotspot interaction: What mid-ocean ridges tell us about deep earth processes, *Oceanography*, v. 20, pp: 102-115.
- Edmonds, H. N., Michael, P. J., Baker, E. T., Graham, D. W., Vock, M., Snow, J., Muhe, R., Connelly, D. P., and German, C. R., Healy 0102 Scientific Party, and ARKVII/2 Scientific Party, Hot springs in a cold ocean: Abundant hydrothermal venting on the ultra-slow-spreading Gakkel Ridge, *Eos Trans. AGU*, 82(47), Fall Meet. Suppl., F647, 2001.
- Escartin, J., and Lin, J., 1995. Ridge offsets, normal faulting, and gravity anomalies of slow spreading ridges, *J. Geophys. Res.*, v.100, pp: 6163-6177.
- Escartin J., Smith, D.K., Cann, J.R., Schouten, H., Langmuir, C.H., and Escrig, S., 2008. Central role of detachment faults in accretion of slow spreading oceanic lithosphere, *Nature* v.455, pp:790-794, doi: 10.1038/nature07333.
- Fisher, A., 2003. In: *Energy and Mass Transfer in Marine Hydrothermal Systems*, Halbach, P.E., Tunnicliffe, V., Hein, J. R., Eds. Dahlem Univ. Press, Berlin, 2003., v. 89, pp. 29–52.
- Fouquet, Y., 1997. Where are the large hydrothermal sulphide deposits in the oceans?, *Royal Soc. London Phil. Trans. Ser. A*, v. 355, pp: 427-441.
- Fox, P.J., Grindlay, N.R., and Macdonald K.C., 1991. The Mid-Atlantic Ridge (31°S-34°30'S): Temporal and spatial variations of accretionary processes, *Mar. Geophys. Res.* v.13, pp:1-20.
- Gac, S., Tisseau, C., Dymont, J., and Goslin, J., 2006. Modelling the thermal evolution of slow-spreading ridge segments and their off-axis geophysical signature. *Geophys. J. Int.*, v.164, pp: 341-358.
- Gamo, T., et al. 1996. Hydrothermal plumes at the Rodriguez triple junction, Indian Ocean, *Earth Planet. Sci. Lett.*, v.142, pp: 261–270, doi :10.1016/0012-821X(96)00087-8.
- Gamo, T., et al. 2001. Chemical characteristics of newly discovered black smoker fluids and associated hydrothermal plumes at the Rodriguez Triple Junction, Central Indian Ridge. *Earth Planet. Sci. Lett.* v.193, pp: 371-379.
- Gente, P., Pockalny, R.A., Durand, C., Deplus, C., Maria, M., Ceuleneer, G., Mevel, C., Cannet, M., Laverne, C., 1995. Characteristics and evolution of the segmentation of the Mid-Atlantic Ridge between 20°N and 24°N during the last 10 million years. *Earth Planet. Sci. Lett.*, v.129, pp: 22-71.
- German, C. R., Baker, E. T., Mevel, C., Tamaki, K., and the FUJI Scientific Team, 1998. Hydrothermal activity along the southwest Indian Ridge, *Nature*, v.395, pp: 490 – 493.
- German, C. R., Yoerger, D. R., Jakuba, M., Shank, T. M., Langmuir, C. H., and Nakamura K., 2008. Hydrothermal exploration with the Autonomous benthic Explorer, *Deep Sea Res.* -I, v. 55, pp: 203-219.
- German, C. R., Bowen, A., Coleman, M. L., Honig, D. L., Huber, J. A., Jakuba, M. V., Kinsey, J. C., Kurz, M. D., Leroy, S., McDermott, J. M., Mercier de Lépinay, B., Nakamura, K., Seewald, J. S., Smith, J. L., Sylva, S. P., Van Dover, C. L., Whitcomb, L. L., and Yoerger, D. R., 2010. Diverse styles of submarine venting on the ultraslow spreading Mid-Cayman Rise, *Proc. Nat. Acad. Sci.*, v.107, pp:14020-14025. doi: 10.1073/pnas.1009205107.
- Gracia, E., J. L. Charlou, J. Radford-Knoery, and L. M. Parson (2000), Non-transform offsets along the Mid-Atlantic Ridge south of the Azores (38°N– 34°N): ultramafic exposures and hosting of hydrothermal vents, *Earth Planet. Sci. Lett.*, v.177, pp: 89– 103.
- Grindlay, N.R., Fox, P.J., and Vogt, P.R., 1992. Morphology and tectonics of the Mid-Atlantic Ridge (25°-27°30'S) from SeaBeam and magnetic data, *J. Geophys. Res.* v. 97, pp: 6983-7010.
- Goslin, J., Triatnord Scientific party, 1999. Extent of Azores plume influence on the Mid-Atlantic Ridge north of hotspot, *Geology* v.27, pp: 991-994.
- Hannington, M.D., Galley, A.G., Herzig, P.M., and Petersen, S., 1998. Comparison of the TAG mound and stock-work complex with Cyprus type massive sulfide deposits; *Proceedings of the Ocean Drilling Program, Scientific Results Volume 158*, College Station, TX, pp: 389-415.
- Hannington, M.D., de Ronde, C.E.J., and Petersen, S., 2005.

- Sea-floor tectonics and submarine hydrothermal systems, in Hedenquist, J.W., et al., eds., *Economic Geology 100th Anniversary Volume*, Society of Economic Geologists, pp: 111-141.
- Hannington, M., Jamieson, J., Monecke, T., Petersen, S., and Beaulieu, S., 2011. The abundance of seafloor massive sulfide deposits, *Geology* 2011, v.39, pp:1155-1158, doi: 10.1130/G32468.1
- Hashimoto, J., Ohta, S., Gamo, T., Chiba, H., Yamaguchi, T., Tsuchida, S., Okudaira, T., Watabe, H., Yamanaka, T., Kitazawa M., 2001. First hydrothermal vent communities from the Indian Ocean discovered, *Zoolog. Sci.*, v.18, pp:717-721, doi:10.2108/zsj.18.717.
- Hey, R.N., Duennebie, F.K., Morgan, W.J., 1980. Propagating rifts on mid-ocean ridges, *J. Geophys. Res.* v. 85, pp: 3647-3658.
- Honsho, C., Tamaki, K. and Fujimoto, H., 1996. Three-dimensional magnetic and gravity studies of the Rodriguez triple junction in the Indian Ocean. *Jour. Geophys. Res.*, v.101, pp: 15877-15848.
- Humphris S.E., Herzig P.M., Miller D.J., Alt J.C., and others, 1995. The internal structure of an active sea-floor massive sulphide deposit, *Nature*, v.377, pp: 713-716.
- IAGA Division V, working group 8, 2000. International Geomagnetic Reference Field, 2000. *Phys. Earth Planet Inter.* v.120, pp: 39-42.
- Jean-Baptiste P, Mantisi F, Pauwells H, Grimaud D and Patriat P, 1992. Hydrothermal 3He and manganese plumes at 19°29'S on the Central Indian ridge, *Geophysical Research Letters*, v.19, pp: 1787-1790.
- Kamesh Raju, K.A., Ramprasad, T and Subrahmanyam, C., 1997. Geophysical investigations over a segment of the Central Indian Ridge Indian Ocean, *Geo-Mar. Lett.* v.17, pp: 195-201.
- Kamesh Raju, K.A., Kodagali, V.N. and Fujimoto, H., 1998. Three dimensional gravity and magnetic studies over a segment of the Carlsberg Ridge, 35th Annual Convention and meeting on Continental Margins of India- Evolution, Processes and Potentials, Indian Geophysical Union, held at NIO, Goa, Nov., 18-20, 1998, P29.
- Kamesh Raju, K.A., Chaubey, A.K., Dileep Amarnath., Abhay Mudholkar., 2008. Morphotectonics of the Carlsberg Ridge between 62°20' and 66°20'E, northwest Indian Ocean. *Mar. Geol.*, v. 252, pp: 120-128.
- Kamesh Raju K.A., Kiranmai Samudrala., Drolia R.K., Dileep A., Ratheesh R. and Mudholkar, A., 2012. Segmentation and morphology of the Central Indian Ridge between 3°S and 11°S, Indian Ocean, *Tectonophysics*, 554-557, pp:114-126. DOI:10.1016/j.tecto.2012.06.001.
- Karson, J.A., 1987. Along-axis variations in seafloor spreading in the MARK area. *Nature* v.328, pp: 681-685.
- Kawagucci, S., Okamura K., Kiyota, K., Tsunogai U., Sano Y., Tamaki K., Gamo T., 2008 Methane, manganese and helium-3 in newly discovered hydrothermal plumes over the Central Indian Ridge, 18°-20°S, *Geochem. Geophys. Geosyst*, 9, Q10002, doi: 10.1029/2008GC002082.
- Kelemen, P.B., Kikawa, E., Miller, D.J., et al., 2004. *Proc. ODP, Init. Repts.*, v.209, 2004.
- Kuo, B.Y., Forsyth, D.W., 1988. Gravity anomalies of the ridge-transform system in the South Atlantic between 31 and 34.5° S: Upwelling centers and variations in crustal thickness, *Mar. Geophys. Res.* v.10, pp: 205-232.
- Lin, J., Purdy, G.M., Schouten, H., Sempere, J.C., Zervas, C., 1990. Evidence from gravity data for focused magmatic accretion along the Mid-Atlantic Ridge, *Nature* v.344, pp: 627-632.
- Lin, J., and Morgan, J.P., 1992. The spreading rate dependence of three-dimensional mid-ocean ridge gravity structure, *J. Geophys. Res. Lett.*, v.19, pp: 13-16.
- Macdonald, K.C., and Luyendyk, B.P., 1977. Deep-tow studies of the structures of the Mid-Atlantic Ridge crest near 37°N (FAMOUS), *Geol. Soc. Am. Bull.*, v.88, pp: 621-636.
- Macdonald, K.C., Miller, S.P., Huestis, S.P., and Spiess, F.N., 1980. Three dimensional modeling of a magnetic reversal boundary from inversion of deep-tow measurements, *J. Geophys. Res.*, v.85, pp: 3670-3680.
- Macdonald, K.C., Fox, P.J., Perram, L.J., Eisen, M. F., Haymon, R.M., Miller, S.P., Carbotte, S.M., Cormier, M. H., and Shor, A.N., 1988. A new view of the Mid-Ocean Ridge from the behavior of ridge axis discontinuities. *Nature* v.335, pp: 217-225.
- Macdonald, K.C., Fox, P.J., 1990. Mid Ocean Ridge. *Sci. Am.* v.262, no.6, pp: 42-49.
- Macdonald, K.C., Scheirer, D.S., Carbotte, S.M., 1991. Mid-Ocean Ridge: Discontinuities, Segments and Giant Cracks, *Science* v.253, pp: 986-994.
- Maia, M., and Gente, P., 1998. Three-dimensional gravity and bathymetry analysis of the Mid-Atlantic Ridge between 20°N and 24°N: Flow geometry and temporal evolution of the segmentation, *J. Geophys. Res.*, v.103, pp: 951-974.
- Marbler, H., A. Koschinsky, T. Pape, R. Seifert, S. Weber, E. T. Baker, L. M. de Carvalho, and K. Schmidt (2010), Geochemical and physical structure of the hydrothermal plume at the ultramafic-hosted Logatchev hydrothermal field at 14°45'N on the Mid-Atlantic Ridge, *Mar. Geol.*, v.271, pp: 187-197.
- McKenzie, D.P., Sclater, J.G., 1971. The evolution of the Indian Ocean since the Late Cretaceous, *Geophys. J. R. Astron. Soc.* v.25, pp: 437-528.
- Mendel, V., Sauter, D., Patriat, P., Munschy, M., 2000. Relationship of the Central Indian Ridge segmentation with the evolution of the Rodriguez triple junction. *Jour. Geophys. Res.*, v.105, pp: 16563-16575.
- Michael, P.J., Langmuir, C.H., Dick, H.C.B., Snow, J.E., Goldstein, S.L., Graham, D.W., Lehnert, K., Kurras, G., Jokat, W., Muhe, R. and Edmonds, H.N., 2003. Magmatic and amagmatic seafloor generation at the ultraslow-spreading Gakkel ridge, Arctic Ocean, *Nature* v.423, pp: 956-961.
- Morishita, T., Hara, K., Nakamura, K., Sawaguchi, T., Tamura, A., Arai, S., Okino, K. and Kumagai, H., 2009. Igneous, alteration and exhumation processes recorded in abyssal

Slow Spreading Ridges of the Indian Ocean: An Overview of Marine Geophysical Investigations

- peridotites and related fault rocks from an oceanic core complex along the Central Indian Ridge. *Jour. Petrol.*, v.50, pp: 1299-1325.
- Mudholkar A.V., Kodagali V.N., Kamesh Raju K.A., Valsangkar A.B., Ranade, G.H. and Ambre N.V., 2002. Geological and geophysical observations along a segment of slow-spreading Carlsberg Ridge, *Curr. Sci.* v.82, pp: 2982-989.
- Münch U., Lalou, C., Halbach, P., and Fujimoto, H., 2001. Relict hydrothermal events along the super-slow Southwest Indian spreading ridge near 63°56'E: Mineralogy, chemistry and chronology of sulfide samples, *Chem. Geol.*, v.177, pp: 341– 349.
- Murton B. J., Baker, E. T., Sands, C. M. and German, C. R., 2006. Detection of an unusually large hydrothermal event plume above the slow-spreading Carlsberg Ridge: NW Indian Ocean., *Geophys Res. Lett.*, v.33, pp: 1-5.
- Nakamura, K., Veirs, S., Sarason, C. P., McDuff, R. E., Stahr, F., Yoerger, D. R., and Bradley A. M., 2000. Electrochemical signals in rising buoyant plumes and tidally oscillating plumes at the main Endeavour vent field, Juan de Fuca Ridge, *Eos Trans.*, 81(48), AGU Fall Meet. Suppl., Abstract OS52I-05.
- Neumann G.A. and Forsyth, D.W., 1993. The paradox of the axial profile: isostatic compensation along the axis of the Mid-Atlantic Ridge?, *J. Geophys. Res.*, v.98, pp: 17891-17910.
- Parker, R.L. and Huestis, S.P. 1974. The inversion of magnetic anomalies in the presence of topography. *J. Geophys. Res.* v.79, pp: 1587-1593.
- Parson, L.M., Patriat, Ph., Searle, R., and Briais, A., 1993. Segmentation of the Central Indian Ridge between 1212'S and Indian Ocean Triple Junction, *Mar. Geophys. Res.*, v.15, pp: 265-282.
- Perfit, M.R., and Chadwick Jr, W.W., 1998. Magmatism at mid-ocean ridges: Constraints from volcanological and geochemical investigations, in: Roger Buck, W., Delaney, T. Paul., Karson, A. Jeffrey, and Lagabriele, Yves, (Eds.), *Faulting and Magmatism at Mid-Ocean Ridges. Geophysical Monograph 106, American Geophysical Union, Washington*, pp: 59-115.
- Phipps Morgan, J. and Forsyth, D.W., 1988. 3-D flow and temperature perturbations due to a transform offset: effects on oceanic crustal and upper-mantle structure, *J. Geophys. Res.*, v.94, pp: 2955-2966.
- Ray, D., Mirza, I. H., Surya Prakash, L., Kaisary, S., Sarma, Y. V. B., Rao, B. R., Somayajulu, Y. K., Drolia, R. K., and KameshRaju K. A., 2008. Water column geochemical anomalies associated with the remnants of a mega plume: A case study after CR-2003 hydrothermal event in Carlsberg Ridge, NW Indian Ocean, *Current Sci.*, v.95, pp: 355-360.
- Ray, D., KameshRaju K. A., Baker, E.T., Srinivas Rao A., Mudholkar A.V., Lupton, J.E., Surya Prakash, L., Gawas, R.B., Vijaya Kumar T. S., 2012. Hydrothermal plumes over the Carlsberg Ridge, Indian Ocean, *Geochem. Geophys. Geosyst.* 13, Q01009, doi: 10.1029/2011GC003888.
- Ray, D., Misra, S, Banerjee, R., 2013. Geochemical variability of MORBs along slow to intermediate spreading Carlsberg-Central Indian Ridge, Indian Ocean. *Jour. Asian Earth Sci.*, 70-71, pp: 125-141.
- Rona, P. A., Widenfalk, L., and Bostrom K., 1987. Serpentinized ultramafics and hydrothermal activity at the Mid-Atlantic Ridge crest near 15°N, *J. Geophys. Res.*,v. 92,pp: 1417-1427.
- Rona, P.A., 2003. Resources of the Sea Floor, *Science*, 299, 673, doi: 10.1126/science.1080679.
- Rona P.A., 2008. The changing vision of marine minerals, *Ore Geology Reviews*, v.33, pp: 618-666.
- Royer, J.Y., Gordon, R.G., 1997. The Motion and Boundary between the Capricorn and Australian Plates. *Science*, v.277, pp: 1268-1274.
- Royer, J.Y., Sclater, J.G., and Sandwell, D.T., 1989. A preliminary tectonic fabric chart of the Indian Ocean, *Proc. Indian Acad. Sci. (Earth and Planet Sci.)*, v.98, pp: 7-24.
- Sandwell, D. T., 1986. Thermal Stress and the Spacing of Transform Faults, *J. Geophys. Res.*, v.91, pp:6405-6418.
- Sandwell, D.T, Smith, W.H.F., 1997. Marine gravity anomaly from geosat and ERS-1 altimetry, *J. Geophys. Res.* v.102, pp: 10039-10054.
- Sauter, D., Nafziger, J.M., Whitechurch, H., 1996. Segmentation and morphotectonic variations of the Central Indian Ridge (21°10'S-22°25'S). *Jour. Geophys. Res.*, v.101, pp: 20233-20256.
- Sauter, D., Patriat, P., Jestin, C.R., Cannet, M., Briais, A., Gallieni Shipboard Scientific Party, 2001. The Southwest Indian Ridge between 49°15'E and 57°E: focused accretion and magma redistribution, *Earth Planet. Sci. Lett.* v.192, pp: 303-317.
- Sempere, J.C., Purdy, G.M., Schouten, H., 1990. The segmentation of the Mid-Atlantic Ridge between 24°N and 30°40'N, *Nature* v.344, pp: 427-431.
- Sempere, J.C., Lin, J., Brown, H.S., Schouten, H., Purdy, G.M., 1993. Segmentation and Morphotectonic variations along a Slow –Spreading Center: The Mid-Atlantic Ridge (24°00'N-30°40'N), *Mar. Geophys. Res.* v.15, pp: 153-200.
- Scheirer, D.S. and Macdonald, K.C., 1993. Variation in cross-sectional area of the axial ridge along the East Pacific Rise: Evidence for the magmatic budget of a fast spreading center, *J. Geophys. Res.*,v. 98, pp: 7871-7885.
- Scheirer D.S., Baker E.T. and Jhonson K.T.M., 1998. Detection of hydrothermal plumes along the Southeast Indian Ridge nears the Amsterdam-St. Paul Plateau, *GRL* v.25, pp: 97-100.
- Schlich, R., 1982. The Indian Ocean: Aseismic ridges, spreading centers, and oceanic basins, in: Nairn A. E. M., and Stehli F. G., (Eds.), *The Ocean Basins and Margins*, vol. 6, The Indian Ocean, Plenum, New York, pp: 51–147.
- Shaw, P.R., 1992. Ridge segmentation, faulting and crustal thickness in the Atlantic Ocean, *Nature* v.358, pp: 490-493.
- Singh, S.C., Crawford, W.C., Carton, H., Seher, T., Combiar, V., Cannat, M., Canales, J.P., Dusunur, D., Escartin, J., and Miranda, J.M., 2006. Discovery of a magma chamber and

- faults beneath a Mid-Atlantic Ridge hydrothermal field, *Nature*, v.442, pp: 1029-1032.
- Sinton, J. M., Detrick, R. S., 1992. Mid-Ocean Ridge Magma Chambers, *J. Geophys. Res.* v.97, pp:197-216.
- Small, C., J. Cochran, J.C. Sempere and D. Christie, The Structure and Segmentation of the Southeast Indian Ridge, **Marine Geology**, 1999.
- Smith, D.K. and Cann, J.R., 1993. Building the Crust at the Mid-Atlantic Ridge, *Nature* v.365, pp: 707-715.
- Smith, W. H. F. and D. Sandwell, 1997. Global seafloor topography from satellite altimetry and ship depth soundings, *Science*, v.277, pp: 1956-1962.
- Snow, J. E., Hellebrand, E., Jokat, W., and Muehe, R., Magmatic and hydrothermal activity in Lena Trough, Arctic Ocean, *EOS Trans. AGU*, 82(17), Spring Meet. Suppl., S193, 2001.
- Son, J., Pak, S.-J., Kim, J., Baker, E. T., You, O.-R., Son, S.-K., Moon and J.W., 2014. Tectonic and magmatic control of hydrothermal activity along the slow-spreading Central Indian Ridge, 8°-17°S, *Geochem. Geophys. Geosyst.*, 15, doi:10.1002/2013GC005206.
- Stein, C.A., and Stein, S., 1994. Constraints on hydrothermal heat flux through the oceanic lithosphere from global heat flow, *Journal of Geophysical Research*, v.99, pp: 3081-3095.
- Tamaki and Shipboard scientists of YK09-13 Leg1 Cruise, 2010. Dodo Field and Solitaire Field: Newly Discovered Hydrothermal Fields at the Central Indian Ridge. Abstract: OS21A-1468, presented at 2010 Fall Meeting, AGU, San Francisco, Calif., 13-17 Dec.
- Tao, C., Lin, J., Guo, S., Chen, J., Wu, G., Han, X., German, C.R., Yoerger, D., Zhou, N., Li, H., Su, X., Zhu, J., and the DY115-19 (Legs 1 -2) and DY115-20 (Legs 4-7) Science Parties, 2012. First active hydrothermal vents on an ultraslow-spreading center: Southwest Indian Ridge, *Geology*, v.40; doi:10.1130/G32389.1
- Tolstoy, M., Harding, A. J., and Orcutt, J.A., 1993. Crustal Thickness on the Mid-Atlantic Ridge Bull's Eye Gravity Anomalies and Focused Accretion, *Science*, v.262, pp: 726-729.
- Tucholke, B.E., Lin, J., Kleinrock, M.C., 1998. Megamullion and mullion structures defining oceanic metamorphic core complexes on the Mid-Atlantic Ridge, *J. Geophys. Res.* v.103, pp: 9857-9866.
- Tucholke, B.E., Behn, M.D., Buck, R.W., Lin, J., 2008. Role of melt supply in oceanic detachment faulting and formation of megamullions, *Geology*, v.36, pp: 455-458.
- Turcotte, D. L., 1974. Are transform faults thermal contraction cracks?, *J. Geophys. Res.*, v.79, pp:2573-2577.
- Van Dover et.al., 2001. Biogeography and ecological setting of Indian Ocean hydrothermal vents, *Science*, v.294, pp: 818-823.
- Vine, F.J. and Matthews, D.H., 1963. Magnetic anomalies over oceanic ridges, *Nature*, v.199, pp:947-949.
- Walker, S. L., Baker, E. T., Resing, J. A., Nakamura, K., and McLain P. D., 2007. A new tool for detecting hydrothermal plumes: An ORP Sensor for the PMEL MAPR, *Eos Trans.* 88(52), AGU Fall Meet. Suppl., Abst. V21D-0753.
- Wessel, P. and Smith, W.H.F., 1991. Free software helps map and display data, *Eos Trans. AGU*, v.72, pp: 445-446.
- Wilson, J. T., 1965. A new class of faults and their bearing on continental drift, *Nature*, v.207, pp: 343-347.
- Wiseman, J.D.H., and Poole, J.H., 1937. Basalts from the Carlsberg Ridge, Indian Ocean. Scientific reports (John Murray Expedition, 1933-34) British Museum of Natural History 30p.



Dr. K.A. Kamesh Raju is working as a Scientist at the CSIR-National Institute of Oceanography (CSIR-NIO), Goa since 1983. Presently he is Chief Scientist. His area of specialization is Marine geophysics with focus on Tectonics and Geodynamics. He has been associated with the Ridge program with a goal to understand the ocean floor tectonics at the dynamic plate boundaries. His other interest is the Andaman Back arc basin in the Andaman Sea. His work has brought out clearly the configuration of the back-arc spreading ridge in the Andaman Sea. He has lead several oceanographic research cruises as the Chief of expedition on board the research vessels ORV Sagar Kanya, RV Sagar Nidhi, RV Sonne and others. He is the recipient of National Mineral Award for the year 2007 for excellence in Applied Geophysics. He is a Life Fellow of the Indian Geophysical Union. He has served as a Steering Committee member of the Inter Ridge, an international scientific organization promoting global mid-Ocean ridge research. He has been awarded with INSA-JSPS fellowship and visited Ocean Research Institute, Tokyo. He has also been invited as visiting scientist by the LDEO, US and IPGP, Paris, France. He is a recognized research guide to supervise Ph.D. thesis in the field of Marine Geophysics by the Andhra and Goa Universities.



Dr. Abhay V. Mudholkar, is working as a Scientist in CSIR-National Institute of Oceanography (CSIR-NIO) since 1983. Presently, he is Chief Scientist and working on the ridge basalts and ultramafic rocks from Carlsberg Ridge as well he is involved in the petrological studies of the Andaman Back-arc basin.



Ms. Kiranmai Samudrala has M.Sc. degree in Marine Geophysics from Andhra University, Visakhapatnam. She is pursuing Ph.D. in Marine Geophysics under Extramural category at Andhra University. Worked at Delta Studies Institute (Andhra University) as a Teaching Assistant. She has qualified CSIR-UGC National Eligibility Test (NET) for Lectureship. Also qualified GATE. She is currently working as Technical Assistant at CSIR-National Institute of Oceanography, Goa.